

# One-Dimensional Conservation Laws with Nonlocal Point Constraints on the Flux



**Boris Andreianov, Carlotta Donadello, Ulrich Razafison,  
and Massimiliano Daniele Rosini**

**Abstract** We review recent results and present new ones on one-dimensional conservation laws with point constraints on the flux. Their application is, for instance, the modeling of traffic flow through bottlenecks, such as exits in the context of pedestrians' traffic and tollgates in vehicular traffic. In particular, we consider nonlocal constraints, which allow to model, e.g., the irrational behavior ("panic") near the exits observed in dense crowds and the capacity drop at tollbooths in vehicular traffic. Numerical schemes for the considered applications, based on finite volume methods, are designed, their convergence is proved, and their validations are done with explicit solutions. Finally, we complement our results with numerical examples, which show that constrained models are able to reproduce important features in traffic flow, such as capacity drop and self-organization.

## 1 Introduction

This chapter deals with macroscopic modeling of traffic flows, both for pedestrians and vehicles, below referred to as agents. The literature on macroscopic models for traffic flows is already vast and characterized by contributions covering statement of problems, modeling aspects, qualitative analysis, and numerical simulations motivated by their real-life applications. Macroscopic models of traffic flows

---

B. Andreianov  
LMPT, CNRS UMR 7350, Université de Tours, Tours, France  
e-mail: [boris.andreianov@lmpt.univ-tours.fr](mailto:boris.andreianov@lmpt.univ-tours.fr)

C. Donadello · U. Razafison  
Laboratoire de Mathématiques CNRS UMR 6623, Université Bourgogne Franche-Comté,  
Besançon, France  
e-mail: [carlotta.donadello@univ-fcomte.fr](mailto:carlotta.donadello@univ-fcomte.fr); [ulrich.razafison@univ-fcomte.fr](mailto:ulrich.razafison@univ-fcomte.fr)

M. D. Rosini (✉)  
Department of Mathematics and Computer Science, University of Ferrara, Ferrara, Italy  
e-mail: [rsnmsm@unife.it](mailto:rsnmsm@unife.it)

are nowadays a consolidated and nonetheless continuously expanding field of mathematical research from both the theoretical and applied point of view, as the surveys [9, 38, 42, 46] and the books [29, 44] demonstrate.

The macroscopic variables (that translate the discrete nature of traffic into continuous variables) are the density of agents  $\rho$ , the velocity  $v$ , and the density flow  $f$ . By definition

$$f = \rho v. \quad (1)$$

Furthermore, the conservation of the number of agents is expressed by the scalar conservation law (CL)

$$\rho_t + f_x = 0. \quad (2)$$

We have to impose a further condition to close system (1), and (2) of two equations and three unknowns. However, (1), and (2) are the only accurate physical laws in traffic flow theory and any other assumption results from an approximation of empirical observations. In fact, traffic modeling cannot be an exact science, e.g., Newtonian physics, because traffic flows are influenced by psychological effects. Nevertheless, good macroscopic models help to understand nontrivial properties of traffic flows, to predict and optimize them.

There are two approaches to close system (1), and (2), which correspond to first- and second-order models. First-order models close system (1), and (2) by expressing one of the three variables in terms of the remaining two. The prototype of the first-order models is the Lighthill, Whitham [35], and Richards [43] (LWR) model, which assumes that the velocity depends on the density alone, namely,  $v = V(\rho)$ . The function  $V$  belongs to  $\mathbf{C}^1([0, \rho_{\max}]; [0, v_{\max}])$  and is non-increasing with  $V(0) = v_{\max}$  and  $V(\rho_{\max}) = 0$ , where  $v_{\max}$  is the maximal speed and  $\rho_{\max}$  is the maximal density. As a result, LWR is expressed by the scalar CL

$$\rho_t + [\rho V(\rho)]_x = 0. \quad (3)$$

Second-order models close system (1), and (2) by adding a CL as third constitutive equation. The most celebrated second-order model is the Aw, Rascle [8], and Zhang [48] model (ARZ). Away from the vacuum  $\rho = 0$ , ARZ writes

$$\begin{pmatrix} \rho \\ y \end{pmatrix}_t + \left[ \begin{pmatrix} y \\ \rho \end{pmatrix} - p(\rho) \begin{pmatrix} \rho \\ y \end{pmatrix} \right]_x = \begin{pmatrix} 0 \\ 0 \end{pmatrix}, \quad (4)$$

where  $y = (v + p(\rho))\rho$  is called generalized momentum. The ‘‘pressure’’ function  $p: \mathbb{R}_+ \rightarrow \mathbb{R}_+$  plays the role of an anticipation factor, taking into account agents’ reactions to the traffic in front of them.

From the modeling point of view, the main drawback of LWR is the fact that agents adjust instantaneously their velocities according to the density they are

experiencing (which implies infinite acceleration) and take into account the slightest change in the density. This behavior contradicts the empirical observations. Also, experimental data show that the fundamental diagram  $(\rho, f)$  is given by a cloud of points rather than being the support of a map  $\rho \mapsto [\rho V(\rho)]$ , see [20, Figure 1.1] or [14, Figure 3.1]. ARZ can be interpreted as a generalization of LWR, possessing a family of fundamental diagram curves, rather than a single one. For this reason ARZ avoids the drawbacks of LWR listed above. Moreover, the empirical tests in [26] show that in many cases, ARZ is significantly more accurate than LWR.

From the mathematical point of view, however, the analysis of ARZ requires a higher degree of technicalities because system (4) degenerates into just one equation at the vacuum. As observed in [31], taking initial data away from the vacuum does not forbid the emergence of vacuum in the solutions; in this case the solutions do not depend continuously on the initial data and experience a sudden increase of the total variation as the vacuum appears.

Goatin [30] bypasses these drawbacks of LWR and ARZ by coupling the two models. The resulting phase transition model (PT) describes the free-flow phase  $\Omega_f$  with LWR and the congested phase  $\Omega_c$  with ARZ. This PT model has been generalized in [10–12, 24].

An underlying assumption of all the models considered above (LWR, ARZ, PT) is that agents move in a homogeneous environment. However, in real life, agents typically move in inhomogeneous spaces characterized by “obstacles” that hinder the density flow, such as bottlenecks and traffic lights. The effect of such obstacles can be represented by introducing point constraints on the density flow

$$f(t, x_i) \leq Q_i \tag{5}$$

at the locations  $x_i$  of obstacles, where  $Q_i$  are their capacities, namely, the maximal density flows allowed through them. The concept of point constraints was first introduced in the framework of crowd dynamics in [23] and in [21] for vehicular traffic. The point constraint (5) is called nonlocal if  $Q_i$  depends in a nonlocal way on the density and local otherwise. We briefly summarize the literature on conservation laws with point constraints recalling that:

- LWR with a local point constraint is studied analytically in [21, 23] and numerically in [7, 16, 19, 22];
- LWR with a nonlocal point constraint is studied analytically in [2, 5] and numerically in [3];
- ARZ with a local point constraint is studied analytically in [6, 25, 28] and numerically in [1];
- PT with a local point constraint is analytically studied in [10, 12, 24].

In the present chapter, we shortly review the above results. For simplicity in the exposition, we consider below only the case of one obstacle placed at  $x = 0$ .

Despite the theory of point constraints is stated in a general mathematical framework (see, for instance, [44, Chapter 6]), according to the authors’ knowledge, it is so far applied only in two frameworks: crowd dynamics [2, 3, 5, 18, 19, 23] and

vehicular traffic [1, 6, 7, 10, 12, 16, 21, 22, 24, 25, 28]. However, it is easy to envisage its application in other fields of research, such as biology (e.g., to model flows of biological substances across cell membranes), biomedicine (e.g., to model blood flows in vessels through thromboses), Internet traffic engineering (e.g., to model flows of data through routers or proxies), etc.

This chapter is organized as follows. Section 2 deals with the Cauchy problem for constrained LWR (3), and (5) in case the constraint is a function of the density, nonlocally both in time and space. The resulting problem is investigated analytically in Sect. 2.1 and numerically in Sect. 2.2. In Sect. 2.3, we construct exact and approximate solutions to some explicit cases. Section 3 deals with the Cauchy problem for constrained ARZ (4), and (5) in case the constraint is a function of time. The well-posedness is then considered in Sect. 3.1. In Sect. 3.2 we construct an exact solution to an explicit case. Section 4 deals with the Cauchy problem for constrained PT (3), (4), and (5) in case the constraint is constant. The well-posedness is then considered in Sect. 4.1. In Sect. 4.2 we construct an exact solution to an explicit case.

## 2 Nonlocally Constrained LWR

In this section we study the Cauchy problem for LWR (3) subject to a point constraint on the density flow (5)

$$\rho_t + f(\rho)_x = 0, \quad x \in \mathbb{R}, t \in (0, T], \quad (6a)$$

$$f(\rho)(t, 0^\pm) \leq Q(t), \quad t \in (0, T], \quad (6b)$$

$$\rho(0, x) = \rho_0(x), \quad x \in \mathbb{R}. \quad (6c)$$

Above  $T > 0$  is the time horizon,  $\rho_0$  is the initial datum, and  $f(\rho) = \rho V(\rho)$  is the flux. Moreover  $Q$  is the maximal density flow allowed through  $x = 0$  and has the form

$$Q(t) = \mathbf{Q}[\rho](t) \text{ for a.e. } t \in [0, T], \quad (7)$$

where the operator

$$\mathbf{Q}: \mathbf{C}^0(0, T; \mathbf{L}^1) \longrightarrow \mathbf{L}^1(0, T)$$

may be nonlocal both in time and space. Above

$$\mathbf{C}^0(0, T; \mathbf{L}^1) = \mathbf{C}^0([0, T]; \mathbf{L}^1(\mathbb{R}; [0, \rho_{\max}])) \quad \text{and}$$

$$\mathbf{L}^1(0, T) = \mathbf{L}^1((0, T); [0, f_{\max}])$$

are, respectively, endowed with the distances induced by the norms

$$\|\rho\|_{\mathbf{C}^0(0,T;\mathbf{L}^1)} = \max_{t \in [0,T]} \int_{\mathbb{R}} |\rho(t, x)| \, dx \text{ and } \|Q\|_{\mathbf{L}^1(0,T)} = \int_0^T |Q(t)| \, dt.$$

### 2.1 Existence and Uniqueness Results

We split the definition of solution to (6), and (7) into two points in the following.

**Definition 1** A couple  $(\rho, Q) \in \mathbf{C}^0([0, T]; \mathbf{L}^1_{\text{loc}}(\mathbb{R}; [0, \rho_{\max}])) \times \mathbf{L}^\infty(0, T)$  is an entropy solution to (6), and (7) if the following conditions hold:

- (i) The function  $\rho$  is an entropy solution of constrained Cauchy problem (6), i.e., for every test function  $\phi \in \mathbf{C}^\infty_c([0, T] \times \mathbb{R}; \mathbb{R}_+)$  and constant  $k \in [0, \rho_{\max}]$

$$\int_{\mathbb{R}} \left[ \int_{\mathbb{R}_+} \left[ |\rho - k| \phi_t + \text{sign}(\rho - k)(f(\rho) - f(k)) \phi_x \right] dt + |\rho_0(x) - k| \phi(0, x) \right] dx \tag{8a}$$

$$+ 2 \int_{\mathbb{R}_+} \left[ 1 - \frac{Q(t)}{\max_{[0, \rho_{\max}]} f} \right] f(k) \phi(t, 0) \, dt \geq 0, \tag{8b}$$

and the left and right traces  $t \mapsto \gamma^\pm f(\rho)(t)$  of  $f(\rho)$  at  $x = 0$  fulfill

$$\gamma^\pm f(\rho)(t) \leq Q(t) \text{ for a.e. } t \in [0, T]. \tag{8c}$$

- (ii) The function  $Q$  is linked to  $\rho$  by relation (7).

Item (i) is precisely [7, Definition 2.1], which is a minor generalization of [21, Definition 3.2]. Line (8a) constitutes the classical Kruzhkov entropy condition (see [33]) suitable for a conservation law without any constraint condition, namely, for (6a), and (6c). Lines (8b) and (8c) account for constraint (6b). Recall that assumption (GNL) given below ensures that the strong traces  $t \mapsto \gamma^\pm \rho(t)$  exist; hence  $f(\rho)(t, 0^\pm)$  coincides with  $f(\rho(t, 0^\pm))$  (see [40]). In the sequel, we write  $f(\rho)(t, 0^\pm)$  for  $\gamma^\pm f(\rho)(t)$  and  $\rho(t, 0^\pm)$  for  $\gamma^\pm \rho(t)$ .

**Definition 2** Two constraint operators  $Q_1$  and  $Q_2$  are equivalent if  $Q_1[\rho] = Q_2[\rho]$  for any entropy solution  $\rho$  of (6), and (7) corresponding to  $Q_1$  or  $Q_2$ .

The existence results for (6), and (7) obtained in [5, 19, 21] rely on the wave-front tracking (WFT) method; see [15, 32] and the references therein. Such method is tailored to the specific expressions of  $Q$  and can be hardly generalized to even slight modification of  $Q$ . For this reason, as in [4], we provide below a rigorous set of

general hypotheses, which guarantee existence and uniqueness of entropy solutions for wide classes of constraint operators, via the application of splitting or fixed-point methods. More precisely, we assume that  $\rho_0$  is in  $\mathbf{L}^1(\mathbb{R}; [0, \rho_{\max}])$  (due to the finite speed of propagation, property for (3), the extension to  $\mathbf{L}^\infty(\mathbb{R}; [0, \rho_{\max}])$  is straightforward; see [5, Theorem 2.1]). On the flux  $f$ , we always assume that

$f$  belongs to  $\mathbf{Lip}([0, \rho_{\max}]; \mathbb{R}_+)$  and is bell – shaped, that is,  $f(0) = 0 = f(\rho_{\max})$  and there exists  $\rho_c \in (0, \rho_{\max})$  such that  $f'(\rho) (\rho_c - \rho) > 0$  (f)  
for a.e.  $\rho \in [0, \rho_{\max}]$ ;

some of our results require the additional assumption

for any  $\rho_1, \rho_2 \in [0, \rho_{\max}]$  such that  $\rho_1 < \rho_2$ , the restriction of  $f$  to  $[\rho_1, \rho_2]$  is not affine. (GNL)

By (f) we have that  $f_{\max} = \max_{[0, \rho_{\max}]} f$  satisfies  $f_{\max} = f(\rho_c)$ . On  $\mathbf{Q}$  we assume that it is “history dependent,” that is

if  $\rho_1, \rho_2 \in \mathbf{C}^0(0, T; \mathbf{L}^1)$  coincide on  $[0, t] \times \mathbb{R}$ , then  $\mathbf{Q}[\rho_1]$  and  $\mathbf{Q}[\rho_2]$  coincide on  $[0, t]$ , (Q<sup>hd</sup>)

and that for any  $t \in [0, T]$  the restriction  $\mathbf{Q}_t : \mathbf{C}^0(0, t; \mathbf{L}^1) \rightarrow \mathbf{L}^1(0, t)$  of  $\mathbf{Q}$  to  $\mathbf{C}^0(0, t; \mathbf{L}^1)$  is such that

$\mathbf{Q}_t$  is Lipschitz continuous, and there exists a non – decreasing map  $\omega \in \mathbf{C}^0(\mathbb{R}_+; \mathbb{R}_+)$  such that  $\omega(0) = 0$  and for any  $\rho_1, \rho_2 \in \mathbf{C}^0(0, T; \mathbf{L}^1)$   
 $\|\mathbf{Q}_t[\rho_1] - \mathbf{Q}_t[\rho_2]\|_{\mathbf{L}^1(0, t)} - \omega(t - \tau) \|\rho_1 - \rho_2\|_{\mathbf{C}^0(0, t; \mathbf{L}^1)} \leq 0$ , (Q<sup>Lip</sup>)  
where  $\tau = \max\{s \in [0, t] : \rho_1 = \rho_2 \text{ in } \mathbf{C}^0(0, s; \mathbf{L}^1)\}$ .

By (Q<sup>hd</sup>) we have that  $\mathbf{Q}_t$ ,  $t \in [0, T]$ , can be defined by letting  $\mathbf{Q}_t[\rho]$  as the restriction to  $[0, t]$  of  $\mathbf{Q}[\mathcal{E}[\rho]]$ , where  $\mathcal{E}[\rho] \in \mathbf{C}^0(0, T; \mathbf{L}^1)$  is an arbitrary extension of  $\rho \in \mathbf{C}^0(0, t; \mathbf{L}^1)$ .

Before stating our main results, let us recall the uniform Lipschitz continuity estimate obtained in [7, Proposition 2.10].

**Lemma 1** *For any  $Q_1, Q_2 \in \mathbf{L}^\infty(0, T)$  and  $t \in [0, T]$ , the corresponding entropy solutions  $\rho_1, \rho_2 \in \mathbf{C}^0(0, t; \mathbf{L}^1)$  to (6) with time horizon  $t$  satisfy*

$$\|\rho_1 - \rho_2\|_{\mathbf{C}^0(0, t; \mathbf{L}^1)} \leq 2 \|Q_1 - Q_2\|_{\mathbf{L}^1(0, t)}.$$

We have the following well-posedness result.

**Theorem 1**

1. If  $\mathbf{Q}$  verifies  $(\mathbf{Q}^{\text{Lip}})$ , then constrained Cauchy problem (6), and (7) admits one and only one entropy solution.
2. The conclusion of 1 still holds true if  $\mathbf{Q}$  is equivalent to a constraint that verifies  $(\mathbf{Q}^{\text{Lip}})$ .

*Proof* By  $(\mathbf{Q}^{\text{Lip}})$  and Lemma 1, the Banach-Picard fixed-point argument yields both existence and uniqueness of solutions on a sufficiently small time interval. Bootstrapping the construction, we achieve the global existence result.

In practice, verification of assumption  $(\mathbf{Q}^{\text{Lip}})$  may be tedious; for this reason we provide the following.

**Proposition 1** *A constraint operator  $\mathbf{Q}$  satisfies  $(\mathbf{Q}^{\text{Lip}})$  if there exists a constant  $C > 0$  such that one of the following conditions is satisfied:*

1. for all  $t \in [0, T]$ ,  $\mathbf{Q}_t$  verifies  $\|\mathbf{Q}[\rho_1] - \mathbf{Q}[\rho_2]\|_{\mathbf{L}^1(0,t)} \leq C \|\rho_1 - \rho_2\|_{\mathbf{L}^1(0,t;\mathbf{L}^1)}$ ;
2. for all  $t \in [0, T]$ ,  $\mathbf{Q}_t$  verifies  $\|\mathbf{Q}[\rho_1] - \mathbf{Q}[\rho_2]\|_{\mathbf{L}^\infty(0,t)} \leq C \|\rho_1 - \rho_2\|_{\mathbf{C}^0(0,t;\mathbf{L}^1)}$ .

While uniqueness seems to require some kind of Lipschitz continuity of  $\mathbf{Q}$ , existence results can be obtained in much more generality. In fact, under assumption  $(\mathbf{GNL})$ , it is enough to require that

$$\mathbf{Q} \text{ can be extended to a continuous map from } \mathbf{L}^1(0, T; \mathbf{L}^1) \text{ to } \mathbf{L}^1(0, T), \quad (\mathbf{Q}^{\text{cont}})$$

whereas if  $(\mathbf{GNL})$  does not hold, then it is enough to require that

$$\mathbf{Q} \text{ is continuous and compact from } \mathbf{C}^0(0, T; \mathbf{L}^1) \text{ to } \mathbf{L}^1(0, T). \quad (\mathbf{Q}^{\text{comp}})$$

Above

$$\mathbf{L}^1(0, T; \mathbf{L}^1) = \mathbf{L}^1((0, T) \times \mathbb{R}; [0, \rho_{\max}]) \text{ and } \mathbf{L}^\infty(0, T) = \mathbf{L}^\infty((0, T); [0, f_{\max}])$$

are, respectively, endowed with the distances induced by the norms

$$\|\rho\|_{\mathbf{L}^1(0,T;\mathbf{L}^1)} = \int_0^T \int_{\mathbb{R}} |\rho(t, x)| \, dx \, dt \quad \text{and} \quad \|\rho\|_{\mathbf{L}^\infty(0,T)} = \text{ess sup}_{t \in (0,T)} |\rho(t)|.$$

More precisely, we have the following existence result.

**Theorem 2** *Constrained Cauchy problem (6), and (7) admits at least one entropy solution if one of the following conditions is satisfied:*

- (a)  $\mathbf{Q}$  satisfies  $(\mathbf{Q}^{\text{comp}})$ .
- (b)  $f$  satisfies  $(\mathbf{GNL})$  and  $\mathbf{Q}$  satisfies  $(\mathbf{Q}^{\text{cont}})$ .

*The same conclusion holds if  $\mathbf{Q}$  is equivalent to a constraint operator that satisfies (a) or (b).*

*Proof* In case (b), compactness of families of functions  $(\rho_\Delta)$  solving (6a) in  $x \neq 0$  is obtained by using the results in [39]. In case (a), compactness of the corresponding  $(Q_\Delta)$  (and consequently that of  $(\rho_\Delta)$ ) is straightforward. In both cases, the Schauder fixed-point argument can be used to resolve the coupling between  $\rho$  and  $Q$  in (6), and (7).

Notice that the embeddings  $\mathbf{L}^1(0, T; \mathbf{L}^1) \supset \mathbf{C}^0(0, T; \mathbf{L}^1)$  and  $\mathbf{L}^\infty(0, T) \subset \mathbf{L}^1(0, T)$  are continuous. Moreover, since the topology of  $\mathbf{L}^1(0, T; \mathbf{L}^1)$  is weaker than that of  $\mathbf{C}^0(0, T; \mathbf{L}^1)$ ,  $(\mathbf{Q}^{\text{cont}})$  and  $(\mathbf{Q}^{\text{comp}})$  are not directly comparable.

In the spirit of Proposition 1, let us point out that the compactness assumption on  $Q$  can follow from the stronger assumption of compactness of  $Q$  as operator from  $\mathbf{C}^0(0, T; \mathbf{L}^1)$  to  $\mathbf{L}^\infty(0, T)$ .

## 2.2 Finite Volume Approximation

In this section we describe the numerical scheme [4] based on finite volume method that we use to solve (6), and (7) and prove its convergence to entropy solutions under the general assumptions  $(\mathbf{Q}_\Delta^{\text{cons}})$  and  $(\mathbf{Q}_\Delta^{\text{comp}})$  given below.

Let  $\Delta x$  and  $\Delta t$  be the constant space and time steps, respectively. Introduce the points  $x_{j+1/2} = j\Delta x$ , the cells  $K_j = [x_{j-1/2}, x_{j+1/2})$  and the cell centers  $x_j = (j - 1/2)\Delta x$  for  $j \in \mathbb{Z}$ . Let  $j_c$  be the index such that  $x_{j_c+1/2}$  is the location of the constraint. Define  $N = \lfloor T/\Delta t \rfloor$  and for  $n \in \mathbb{N} \cap [0, N]$  introduce the time discretization  $t^n = n\Delta t$ . For  $n \in \mathbb{N} \cap [0, N]$  and  $j \in \mathbb{Z}$ , we denote by  $\rho_j^n$  the approximation of the average of  $\rho(t^n, \cdot)$  on the cell  $K_j$ , namely

$$\rho_j^0 = \frac{1}{\Delta x} \int_{K_j} \rho_0(x) dx \quad \text{and} \quad \rho_j^n \simeq \frac{1}{\Delta x} \int_{K_j} \rho(t^n, x) dx \quad \text{if } n > 0.$$

The discretized initial datum  $\rho_\Delta^0$  is defined by

$$\rho_\Delta^0(x) = \rho_j^0 \quad \text{for } x \in K_j, \quad (9)$$

converges to  $\rho_0$  in  $\mathbf{L}^1(\mathbb{R})$  and obeys the same  $\mathbf{L}^\infty$  bounds as  $\rho_0$ .

Let  $(\rho_\Delta, Q_\Delta): [0, T] \times \mathbb{R} \rightarrow [0, \rho_{\max}] \times [0, f_{\max}]$  be an approximate solution with

$$\rho_\Delta(t, x) = \sum_{n=1}^N \rho_\Delta^n(x) \chi_{(t^{n-1}, t^n]}(t), \quad Q_\Delta(t) = \sum_{n=1}^N Q_\Delta^n \chi_{(t^{n-1}, t^n]}(t),$$

where  $(\rho_\Delta^n, Q_\Delta^n)$  is a discrete function computed by executing the following algorithm, based on a suitable discretization  $Q_\Delta$  of  $Q$  that satisfies  $(\mathbf{Q}^{\text{hd}})$ .



0. Initialization. We start with  $\rho_\Delta^0$  given in (9) and  $Q_\Delta^0 = \mathbf{Q}_\Delta[\rho_\Delta^0](0)$ .

1. For each  $n \in [0, N - 1] \cap \mathbb{N}$ ,

A. A finite volume method [7] for constrained Cauchy problem (6) is

$$\rho_j^{n+1} = \rho_j^n - \frac{\Delta t}{\Delta x} \left( \mathcal{F}_{j+1/2}^n - \mathcal{F}_{j-1/2}^n \right), \quad (10)$$

where

$$\mathcal{F}_{j+1/2}^n = \begin{cases} \mathfrak{F}(\rho_j^n, \rho_{j+1}^n) & \text{if } j \neq j_c, \\ \min \left\{ \mathfrak{F}(\rho_j^n, \rho_{j+1}^n), Q_\Delta^n \right\} & \text{if } j = j_c, \end{cases} \quad (11)$$

is a monotone, consistent numerical flux, namely

- $\mathfrak{F} \in \mathbf{Lip}([0, \rho_{\max}]^2; \mathbb{R})$  with Lipschitz constant  $\mathbf{Lip}(\mathfrak{F})$ ,
- $\mathfrak{F}(a, a) = f(a)$  for any  $a \in [0, \rho_{\max}]$ ,
- $[0, \rho_{\max}]^2 \ni (a, b) \mapsto \mathfrak{F}(a, b) \in [0, f_{\max}]$  is non-decreasing with respect to  $a$  and non-increasing with respect to  $b$ ,

and  $Q_\Delta^n$  is an approximation of  $Q(t^n)$ .

B. Given  $(\rho_\Delta^k)_{k=1, \dots, n}$  with  $\rho_\Delta^n(x) = \rho_j^n$  for  $x \in K_j$ , we compute  $Q_\Delta^n \in [0, f_{\max}]$  by discretizing relation (7):

$$Q_\Delta^n = \mathbf{Q}_\Delta[\mathcal{E}^n[\rho_\Delta^n]](t^n), \quad (12)$$

where  $\mathcal{E}^n[\rho_\Delta^n](t, x) = \sum_{k=1}^n \rho_\Delta^k(t - t^{k-1}, x) \mathbf{1}_{(t^{k-1}, t^k]}(t)$ .

We use the  $\mathbf{L}^1(0, T)$ -norm for  $Q_\Delta$  and with the  $\mathbf{L}^\infty(0, T; \mathbf{L}^1)$ -norm for  $\rho_\Delta$ , both norms being computed from the above expressions of  $Q_\Delta$  and  $\rho_\Delta$  as functions of  $t$  and  $(t, x)$ , respectively.

In the following we assume that the approximations of  $\mathbf{Q}$  given by  $\mathbf{Q}_\Delta$  are consistent

$$\left. \begin{array}{l} \|Q_\Delta - Q\|_{\mathbf{L}^1(0, T)} \rightarrow 0 \\ \|\rho_\Delta - \rho\|_{\mathbf{L}^1(0, T; \mathbf{L}^1)} \rightarrow 0 \\ Q_\Delta = \mathbf{Q}_\Delta[\rho_\Delta] \end{array} \right\} \implies Q = \mathbf{Q}[\rho] \quad (\mathbf{Q}_\Delta^{\text{cons}})$$

and the following asymptotic compactness property

$$\left. \begin{array}{l} (\rho_\Delta) \text{ is bounded in } \mathbf{L}^\infty(0, T; \mathbf{L}^1) \\ Q_\Delta = \mathbf{Q}_\Delta[\rho_\Delta] \end{array} \right\} \implies (Q_\Delta) \text{ is compact in } \mathbf{L}^1(0, T). \quad (\mathbf{Q}_\Delta^{\text{comp}})$$

Here and in the sequel, by compactness of  $(Q_\Delta)$ , we mean the possibility to extract a convergent subsequence in  $\mathbf{L}^1(0, T)$ , i.e., the relative compactness.

As in [7, Proposition 4.2], under the CFL condition

$$\text{Lip}(\mathfrak{F}) \frac{\Delta t}{\Delta x} \leq \frac{1}{2},$$

we have the  $\mathbf{L}^\infty$ -stability of the scheme (10), (11), and (12), that is

$$0 \leq \rho_\Delta(t, x) \leq \rho_{\max} \quad \text{for a.e. } (t, x) \in (0, T) \times \mathbb{R}.$$

We have the following convergence results of our scheme.

**Theorem 3** *Let  $\mathbf{Q}$  verify  $(\mathbf{Q}^{\text{Lip}})$  and  $(\rho, Q)$  be the unique entropy solution of (6), and (7).*

1. *If  $\mathbf{Q}$  admits an approximation  $\mathbf{Q}_\Delta$  that satisfies  $(\mathbf{Q}_\Delta^{\text{cons}})$  and  $(\mathbf{Q}_\Delta^{\text{comp}})$ . Then  $(\rho_\Delta, Q_\Delta)$  constructed by the scheme (10), (11), and (12) converges to  $(\rho, Q)$  as  $\Delta t, \Delta x \rightarrow 0$ .*
2. *The conclusion of 1. still holds true if  $\mathbf{Q}$  is equivalent to a constraint that verifies  $(\mathbf{Q}^{\text{Lip}})$  and admits an approximation that satisfies  $(\mathbf{Q}_\Delta^{\text{cons}})$  and  $(\mathbf{Q}_\Delta^{\text{comp}})$ , then the approximate solution constructed by the corresponding scheme (10), (11), and (12) converges to  $(\rho, Q)$  as  $\Delta t, \Delta x \rightarrow 0$ .*

### 2.3 Examples

In this section we give some examples of constraint operators satisfying the hypothesis of Theorem 1. This means that the associated constrained Cauchy problems are well-posed. Below  $q \in \mathbf{Lip}([0, \rho_{\max}]; (0, f_{\max}])$  is non-increasing,  $w \in \mathbf{L}^\infty(\mathbb{R}_-; \mathbb{R}_+)$  is non-decreasing with  $\|w\|_{\mathbf{L}^1(\mathbb{R}_-)} = 1$  and  $\text{supp}(w) = [-i_w, 0]$ ,  $i_w > 0$ ,  $\kappa \in \mathbf{Lip}(\mathbb{R}_+; \mathbb{R}_+)$  is non-increasing with  $\|\kappa\|_{\mathbf{L}^1(\mathbb{R}_+)} = 1$  and  $\text{supp}(\kappa) = [0, \tau]$ ,  $\tau > 0$ , which express the dependence of the constraint level on the subjective density, the space non-locality, and the time non-locality (memory), respectively. We also assume that  $w$  belongs to  $\mathbf{Lip}((-\infty, 0); \mathbb{R}_+)$  but can be/is discontinuous at  $x = 0$ . The numerical simulations are performed using the Ruzanov fux [45]:

$$\mathfrak{F}(a, b) = \frac{f(a) + f(b)}{2} - \frac{b - a}{2} \max(|f'(a)|, |f'(b)|).$$

*Example 1* If  $w \in \mathbf{C}_c^1(\mathbb{R}; \mathbb{R}_+)$  and  $\mathfrak{K} \in \mathbf{C}^2(\mathbb{R}_+; \mathbb{R}_+)$  is the primitive of  $\kappa$  such that  $\mathfrak{K}(0) = 0$ , then the nonlocal (both in time and space) constraint operators

$$\mathbf{Q}_1[\rho](t) = q \left( \int_{\mathbb{R}_-} \int_0^t w(x) \kappa(t - s) \rho(s, x) \, ds \, dx \right), \quad (13)$$

$$\begin{aligned} \mathbf{Q}_2[\rho](t) = q \left( \int_{\mathbb{R}_-} \left[ w(x) \mathfrak{K}(t) \rho_0(x) + w'(x) \int_0^t \mathfrak{K}(t-s) f(\rho)(s, x) ds \right] dx \right. \\ \left. - w(0^-) \int_0^t \mathfrak{K}(t-s) f(\rho)(s, 0^-) ds \right), \end{aligned} \tag{14}$$

are well defined and equivalent. Such operators correspond to the case of a maximal density flow at  $x = 0$  which depends on the values of  $\rho$  in  $\text{supp}(\kappa(t - \cdot)) \times \text{supp}(w)$ . The monotonicity assumption on  $w$  (on  $\kappa$ ) implies that the capacity is more affected by the “closest” (“more recent”) values of  $\rho$ . Let also

$$\mathbf{Q}_3[\rho](t) = q \left( \sum_{0 < t_i \leq t} [t_i - t_{i-1}] \kappa(t - t_{i-1}) \left[ \int_{\mathbb{R}_-} w(x) \rho(t_i, x) dx \right] \right), \tag{15}$$

$$\mathbf{Q}_4[\rho](t) = q \left( \sum_{y_i < 0} [y_{i+1} - y_i] w(y_i) \left[ \int_0^t \kappa(t-s) \rho(s, y_{i+1}) ds \right] \right), \tag{16}$$

which are discretized versions of  $\mathbf{Q}_1$ , with  $t_i < t_{i+1}$  and  $y_0 \leq y_i < y_{i+1} \leq y_{M+1} = 0$ .

Such operators can model, for instance, the traffic through tollbooths if the number of open gates is decided according to online data. One might think that both  $\mathbf{Q}_1$  and  $\mathbf{Q}_2$  correspond to data collected by a video camera registering the area given by  $\text{supp}(w)$ ,  $\mathbf{Q}_3$  corresponds to data collected by a photo camera that shoots photos at times  $t_i$  of the area given by  $\text{supp}(w)$ , and  $\mathbf{Q}_4$  corresponds to data collected by local sensors located at  $y_i$ . In each of these cases,  $\text{supp}(\kappa)$  is the period of time the data are taken into account.

In Fig. 1 we represent the exact solution  $\rho$  corresponding to the constraint operator  $\mathbf{Q}_1$ ,  $f(\rho) = (1 - \rho) \rho$  (hence  $v_{\max} = 1$  and  $\rho_{\max} = 1$ ),  $w(x) = 2(1 + x) \chi_{[-1,0]}(x)$ ,  $\kappa(t) = 2(1 - t) \chi_{[0,1]}(t)$ ,  $\rho_0(x) = \chi_{[-6,-1.2]}(x)$  and

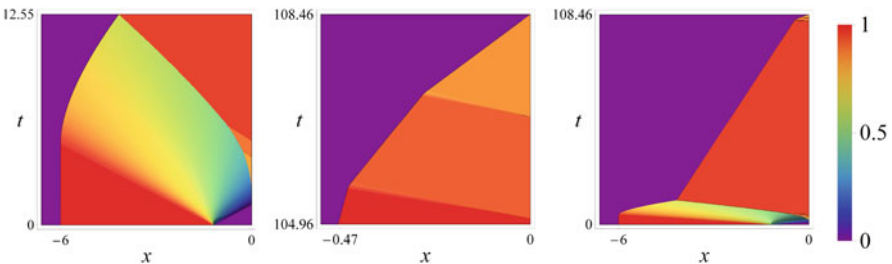
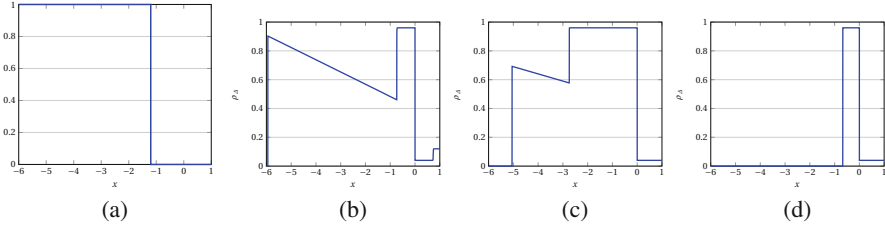


Fig. 1 The solution  $\rho$  described in Example 1



**Fig. 2** The approximate solution  $x \mapsto \rho_\Delta(t, x)$  at different times for  $\Delta x = 10^{-3}$  and  $\Delta t = 4 \times 10^{-4}$ . (a)  $\rho_\Delta(0, x)$ . (b)  $\rho_\Delta(5.878, x)$ . (c)  $\rho_\Delta(10, x)$ . (d)  $\rho_\Delta(100, x)$

**Table 1** Relative  $\mathbf{L}^1$ -error at time  $t = 10$ , for the constraints  $\mathbf{Q}_1$  and  $\mathbf{Q}_2$

Space step	$\mathbf{Q}_1$ defined in (13)		$\mathbf{Q}_2$ defined in (14)	
	$\mathbf{L}^1$ -error	Rate of convergence	$\mathbf{L}^1$ -error	Rate of convergence
600	$9.68 \times 10^{-3}$	–	$1.07 \times 10^{-2}$	–
1200	$5.06 \times 10^{-3}$	0.935	$5.64 \times 10^{-3}$	0.923
2400	$2.73 \times 10^{-3}$	0.913	$3.03 \times 10^{-3}$	0.91
6000	$1.24 \times 10^{-3}$	0.891	$1.37 \times 10^{-3}$	0.892
12000	$6.56 \times 10^{-4}$	0.892	$7.28 \times 10^{-4}$	0.892
24000	$3.36 \times 10^{-4}$	0.902	$3.8 \times 10^{-4}$	0.898

$$q(\xi) = \begin{cases} q_0 & \text{if } 0 \leq \xi < \xi_1, \\ q_1 & \text{if } \xi_1 \leq \xi < \xi_2, \\ q_2 & \text{if } \xi_2 \leq \xi \leq 1, \end{cases} \quad (17)$$

with  $q_0 = 0.16$ ,  $q_1 = 0.1056$ ,  $q_2 = 0.0384$ ,  $\xi_1 \sim 0.508$ ,  $\xi_2 \sim 0.6911$ . The approximate solution  $x \mapsto \rho_\Delta(t, x)$  is represented at different fixed times  $t$  in Fig. 2. Table 1 lists the relative  $\mathbf{L}^1$ -errors

$$\left[ \sum_j \left| \rho(t^n, x_j) - \rho_j^n \right| \right] / \left[ \sum_j \left| \rho(t^n, x_j) \right| \right]$$

at time  $t^n = 10$  between the exact and approximate solutions computed with the constraint operators  $\mathbf{Q}_1$  and  $\mathbf{Q}_2$  for different numbers of space cells and for a fixed time step  $\Delta t = 10^{-4}$ . The relative  $\mathbf{L}^1$ -errors are similar; hence the solutions corresponding to  $\mathbf{Q}_1$  and  $\mathbf{Q}_2$  are essentially the same, and in fact  $\mathbf{Q}_1$  and  $\mathbf{Q}_2$  are very close to one another. This is not surprising, indeed, the constraint operators  $\mathbf{Q}_1$  and  $\mathbf{Q}_2$  are equivalent in the sense of Definition 2. We recall that equivalent constraints lead to the same solutions. Thus, the schemes based on the respective discretizations of  $\mathbf{Q}_1$  and  $\mathbf{Q}_2$  should be seen as different approximations of one and the same continuous problem.

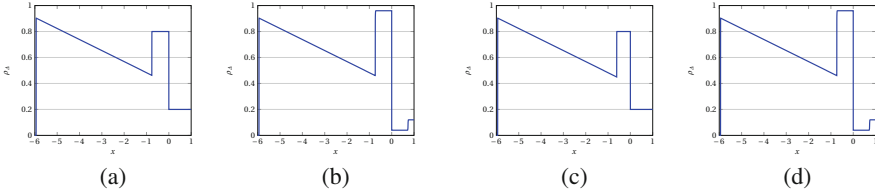


**Fig. 3** Solutions  $x \mapsto \rho_{\Delta}(10, x)$  corresponding to  $\mathbf{Q}_3$  and  $\mathbf{Q}_4$  for  $\Delta x = 10^{-3}$  and  $\Delta t = 4 \times 10^{-4}$ . **(a)**  $x \mapsto \rho_{\Delta}(5.878, x)$  for  $t_0 = 0, t_1 = 2$  and  $t_3 = 5$ . **(b)**  $x \mapsto \rho_{\Delta}(5.878, x)$  for all  $t_i = i \Delta t, i = 0, \dots, 14695$ . **(c)**  $x \mapsto \rho_{\Delta}(5.878, x)$  for  $y_0 = -1.1$  and  $y_1 = 0$ . **(d)**  $x \mapsto \rho_{\Delta}(5.878, x)$  for all  $y_i = -6 + i \Delta x, i = 1, \dots, 7000$

We focus on the constraint operators  $\mathbf{Q}_3$  and  $\mathbf{Q}_4$ . For each of them, we perform two types of simulations: one by taking a small number of discretized times or positions (see Fig. 3a, c) and one by taking all the times and positions of the discretization (see Fig. 3b, d). Notice a good agreement between Fig. 3b, d, and Fig. 2c. As expected, the constraint operator that corresponds to the case where data are collected by a video camera is the more efficient since the two other may underestimate the importance of the congestion before the exit.

*Example 2* The *capacity drop* of a bottleneck when a high density accumulates upstream is reproduced in [5] by the constraint operator

$$\mathbf{Q}_1[\rho](t) = q(\Xi^1(t)), \quad \Xi^1(t) = \int_{\mathbb{R}_-} w(x) \rho(t, x) dx, \quad (18)$$

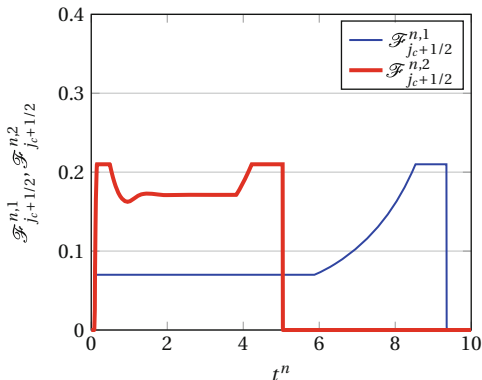
where  $\Xi^1$  is *subjective density* at the bottleneck. Existence and uniqueness results for this model are proved in [5, Theorem 3.1]. Since  $(\mathbf{Q}^{\text{hd}})$  is obvious and  $(\mathbf{Q}^{\text{Lip}})$  follows from Proposition 1, thanks to Theorem 1 we can give a shorter alternative proof, which requires weaker hypotheses on  $q$  and  $w$ . However this proof does not give any hint on the behavior of the entropy solution nor a priori bounds of its total variation, unlike to the (much longer) arguments of [5]. Observe that we do not need to assume  $(\mathbf{GNL})$ .

According to this model, even a small density may form a queue provided a sufficiently high density is approaching from behind. This drawback is tempered by considering a memory effect and choosing  $\mathbf{Q}_2[\rho](t) = q(\Xi^2(t))$  with

$$\Xi^2(t) = \min \left\{ \int_{\mathbb{R}_-} w(x) \rho(t, x) dx, \alpha f_-^{-1} \left( \int_0^t \kappa(t-s) f(\rho)(s, 0^-) ds \right) \right\}, \quad (19)$$

being  $\alpha \in (0, \rho_{\max}/\rho_c)$  a constant and  $f_-$  the restriction of  $f$  to  $[0, \rho_c]$ . Indeed, if, for instance,  $\alpha = \sqrt{5}$ , the numerical domain is  $[-6, 1]$ ,  $f(\rho) = (1 - \rho^2)^2 \rho$ ,  $\rho_0(x) = \chi_{[-1, -0.1]}(x)$  and

**Fig. 4** The fluxes at the exit  $\mathcal{F}_{j_c+1/2}^{n,1}$  and  $\mathcal{F}_{j_c+1/2}^{n,2}$  corresponding to the constraints (18) and (19), respectively, for  $\Delta x = 10^{-3}$  and  $\Delta t = 4 \times 10^{-4}$



$$q(\xi) = \begin{cases} q_0 & \text{if } 0 \leq \xi < \xi_1, \\ \frac{(q_0 - q_1)\xi + q_1\xi_1 - q_0\xi_2}{\xi_1 - \xi_2} & \text{if } \xi_1 \leq \xi < \xi_2, \\ q_1 & \text{if } \xi_2 \leq \xi \leq 1, \end{cases}$$

with  $q_0 = 0.21$ ,  $q_1 = 0.07$ ,  $\xi_1 = 0.3$ ,  $\xi_2 = 0.7$ , then, at least in this case, the constraint operator (19) does not present the drawback pointed out for the constraint operator (18); see Fig. 4. Moreover, Fig. 4 shows that the constraint operator (19) qualitatively reproduces also the self-organization. Indeed, the flux in red first increases until it reaches the maximum level of the efficiency of the exit, and then it falls down, and after a very short period, it increases without reaching the maximum level of the efficiency: this is the effect of self-organization [17, 47].

A further drawback of (18) is that it does not take into account memory effects of inertia kind; in fact  $\Xi^1$  is the solution of the ordinary differential equation (ODE)

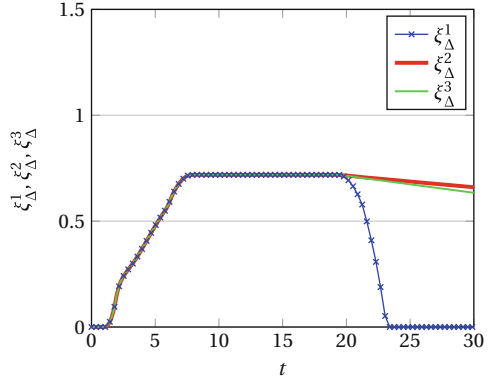
$$\dot{\Xi}(t) = \int_{\mathbb{R}_-} w'(x)[f(\rho)(t, x) - f(\rho)(t, 0^-)]dx,$$

hence  $\Xi^1$  uniquely depends on the instantaneous values of  $\rho$ . This drawback is tempered by choosing  $\Xi^3$  or  $\Xi^4$  solutions in  $\mathcal{D}'([0, T])$  of the Cauchy problems for ODEs

$$\Xi^3: \begin{cases} \dot{\Xi}(t) = \max \left\{ \int_{\mathbb{R}_-} w'(x)[f(\rho)(t, x) - f(\rho)(t, 0^-)]dx, -\delta \Xi(t) \right\}, \\ \Xi(0) = \Xi_0[\rho_0], \end{cases} \tag{20}$$

$$\Xi^4: \begin{cases} \dot{\Xi}(t) = \max \left\{ \int_{\mathbb{R}_-} w'(x)[f(\rho)(t, x) - f(\rho)(t, 0^-)]dx, -\delta \right\}, \\ \Xi(0) = \Xi_0[\rho_0], \end{cases} \tag{21}$$

**Fig. 5** The approximate functions  $\Xi_{\Delta}^1, \Xi_{\Delta}^3, \Xi_{\Delta}^4$  of  $\Xi^1, \Xi^3, \Xi^4$  defined in (18), (20), and (21) for  $\Delta x = 10^{-3}$  and  $\Delta t = 4 \times 10^{-4}$



where  $\Xi_0: \mathbf{L}^1(\mathbb{R}) \rightarrow \mathbb{R}$  and  $\delta > 0$  is a constant. Indeed, if  $\delta = 8 \times 10^{-3}$ , the numerical domain is  $[-6, 1]$ ,  $f(\rho) = (1 - \rho^2)^2 \rho$ ,  $\rho_0(x) = \chi_{[-5.75, -2]}(x)$ ,  $q$  is given by (17) with  $q_0 = 0.21, q_1 = 0.168, q_2 = 0.021, \xi_1 = 0.566, \xi_2 = 0.731$ , then, at least in this case, the constraint operators associated to (20) and (21) do not present the drawback pointed out for the constraint operator (18); see Fig. 5.

### 3 Locally Constrained ARZ

This section is devoted to the study of ARZ (4)

$$\begin{pmatrix} \rho \\ y \end{pmatrix}_t + \left[ \begin{pmatrix} y \\ \rho \end{pmatrix} - p(\rho) \right] \begin{pmatrix} \rho \\ y \end{pmatrix}_x = \begin{pmatrix} 0 \\ 0 \end{pmatrix}, \tag{22}$$

where the density  $\rho$  and the generalized momentum  $y$  are such that  $(\rho, y)$  belongs to  $\mathcal{B} = \{(\rho, y) \in \mathbb{R}_+^2 : 0 \leq \rho p(\rho) \leq y\}$ . Recall that  $p: \mathbb{R}_+ \rightarrow \mathbb{R}_+$  accounts agents' reactions to the state of traffic in front of them. We assume that  $p$  belongs to  $\mathbf{C}^0(\mathbb{R}_+; \mathbb{R}_+) \cap \mathbf{C}^2((0, \infty); \mathbb{R}_+)$  and satisfies

$$p(0) = 0, \quad p'(\rho) > 0 \quad \text{and} \quad p'(\rho) + \rho p''(\rho) > 0 \quad \text{for every } \rho > 0,$$

$$\lim_{\rho \downarrow 0} [\rho^2 p'(\rho)] = 0, \quad \lim_{\rho \downarrow 0} \left| \frac{\rho p''(\rho)}{p'(\rho)} \right| < \infty.$$

Typical choice is  $p(\rho) = \rho^\gamma, \gamma > 0$ ; see [8].

ARZ can be interpreted as a generalization of LWR, possessing a fundamental diagram  $(\rho, f)$  which is a two-dimensional manifold rather than a one-dimensional manifold as for LWR. This is consistent with experimental data (see, for instance, [20, Figure 1.1] or [14, Figure 3.1]), according to which the fundamental diagram  $(\rho, f)$  is given by a cloud of points rather than being the support of a map  $\rho \mapsto V(\rho) \rho$ .

To any Lagrangian marker  $w = y/\rho$ , we can associate the fundamental diagram curve  $\rho \mapsto (w - p(\rho))\rho$ , which has maximal slope  $w$  and intersects  $f = 0$  at the vacuum  $\rho = 0$  and at  $\rho = p^{-1}(w)$ . Since  $w = w(t, x)$  satisfies the equation  $w_t + v w_x = 0$ , the vehicle initially at  $x_0 \in \mathbb{R}$  is characterized at any time  $t > 0$  by the Lagrangian marker  $w(0, x_0)$  and has, therefore, maximal speed  $w(0, x_0)$  and length  $1/p^{-1}(w(0, x_0))$ . For this reason, ARZ can also be interpreted as a generalization of LWR to the case of a multi-population traffic.

Away from the vacuum, system (22) is strictly hyperbolic,  $\lambda_1 < \lambda_2$ , the first characteristic field is genuinely nonlinear,  $\nabla \lambda_1 \cdot R_1 < 0$ , and the second characteristic field is linearly degenerate,  $\nabla \lambda_2 \cdot R_2 = 0$ , where  $\lambda_1 = \frac{y}{\rho} - p(\rho) - \rho p'(\rho)$ ,  $\lambda_2 = \frac{y}{\rho} - p(\rho)$  are the eigenvalues of the Jacobian matrix of the flux and  $R_1 = (\rho, y)$ ,  $R_2 = (\rho, y + \rho^2 p'(\rho))$  are the corresponding eigenvectors.

At the vacuum, system (22) degenerates into just one equation. In particular, the solutions to (22) fail to depend continuously on the initial data in any neighborhood of  $\rho = 0$  (see [8]); moreover, the solutions may experience a sudden increase of the total variation as the vacuum appears (see [31]).

A theory for traffic flow away from the vacuum is not of practical interest. Indeed, a trivial example of vacuum formation is downstream of a traffic light when it is red. Moreover, vacuum might appear even without the action of a traffic light when, for instance, slow and fast vehicles initially in  $(-\infty, 0]$  and  $(0, \infty)$ , respectively, move at their maximal speed. For this reason we extend the flux to the vacuum by introducing  $F: \mathcal{Y} \rightarrow \mathbb{R}_+$  defined by

$$F(\rho, y) = \begin{cases} (0, 0) & \text{if } \rho = 0, \\ \left[ \frac{y}{\rho} - p(\rho) \right] (\rho, y) & \text{if } \rho \neq 0. \end{cases}$$

Moreover, we introduce the change of variables

$$\rho = \tau(v, w), \quad y = \tau(v, w) w,$$

where the components of  $(v, w)$  are the Riemann invariant coordinates (velocity and Lagrangian marker, respectively) and  $\tau(v, w) = p^{-1}(w - v)$ . The main motivation for this change of variables stems from the fact that the total variation of the solutions in these coordinates does not increase; see [27, 31, 37] where this property is exploited to prove existence results for ARZ. Furthermore, at the vacuum, the entropy pairs defined below in (24) are well defined in the  $(v, w)$  coordinates and multivalued in the  $(\rho, y)$  coordinates.

In the new variables,  $\mathcal{Y}$  becomes  $\mathcal{W} = \{(v, w) \in \mathbb{R}_+^2 : v \leq w\}$ . Notice that the vacuum  $\rho = 0$  corresponds in the  $(\rho, y)$  variables to the point  $(\rho, y) = (0, 0)$  and in the  $(v, w)$  variables to the half line  $\mathcal{W}_0 = \{(v, w) \in \mathcal{W} : v = w\}$ . Let  $\mathcal{W}_0^c = \mathcal{W} \setminus \mathcal{W}_0$  be the set of the non-vacuum states.



The Cauchy problem for ARZ (22) subject to a point constraint on the density flow (5) writes in the new variables

$$Y(v, w)_t + F(Y(v, w))_x = (0, 0), \quad x \in \mathbb{R}, t \in (0, T], \quad (23a)$$

$$f(v, w)(t, 0^\pm) \leq Q(t), \quad t \in (0, T], \quad (23b)$$

$$(v, w)(0, x) = (v_0, w_0)(x), \quad x \in \mathbb{R}, \quad (23c)$$

where  $T > 0$  is the time horizon,  $Y(v, w) = (\mathfrak{r}(v, w), \mathfrak{r}(v, w) w)$ ,  $(v_0, w_0) \in \mathbf{L}^\infty(\mathbb{R}; \mathscr{W})$  is the initial datum,  $Q(t)$  is the maximal density flow allowed at  $x = 0$  at time  $t > 0$ , and  $f(v, w) = \mathfrak{r}(v, w) v$ .

### 3.1 Existence and Uniqueness Results

Before stating the definition of entropy solution to (23), we introduce the family of entropy-entropy flux pairs

$$E_k(v, w) = \begin{cases} 0 & \text{if } v \leq k, \\ 1 - \frac{p^{-1}(w-v)}{p^{-1}(w-k)} & \text{if } v > k, \end{cases} \quad F_k(v, w) = \begin{cases} 0 & \text{if } v \leq k, \\ k - \frac{f(v,w)}{p^{-1}(w-k)} & \text{if } v > k, \end{cases} \quad (24)$$

and the ‘‘compensation term’’

$$N_k(v, w, Q) = \begin{cases} f(v, w)(t, 0) \left[ \frac{k}{Q(t)} - \frac{1}{p^{-1}(|w(t,0)-k|^+)} \right]^+ & \text{if } Q(t) \neq 0, \\ k & \text{otherwise.} \end{cases}$$

**Definition 3** We say that  $(v, w) \in \mathbf{L}^\infty(\mathbb{R}_+; \mathbf{BV}(\mathbb{R}; \mathscr{W})) \cap \mathbf{C}^0(\mathbb{R}_+; \mathbf{L}^1_{\text{loc}}(\mathbb{R}; \mathscr{W}))$  is a constrained entropy solution to (23) if the following conditions hold:

- (i)  $(v, w)$  is a weak solution of Cauchy problem (23a), and (23c), i.e.,  $(v, w)(0, x) = (v_0, w_0)(x)$  for a.e.  $x \in \mathbb{R}$  and for any test function  $\phi \in \mathbf{C}^\infty_c((0, \infty) \times \mathbb{R}; \mathbb{R})$

$$\iint_{\mathbb{R}_+ \times \mathbb{R}} \mathfrak{r}(v, w) [\phi_t + v \phi_x] (1, w) dx dt = (0, 0).$$

- (ii)  $(v, w)$  satisfies constraint (23b), namely,  $f(v, w)(t, 0^\pm) \leq Q(t)$  for a.e.  $t > 0$  and for any test function  $\phi \in \mathbf{C}^\infty_c((0, \infty) \times \mathbb{R}; \mathbb{R}_+)$  and constant  $k > 0$

$$\iint_{\mathbb{R}_+ \times \mathbb{R}} [E_k(v, w) \phi_t + F_k(v, w) \phi_x] dx dt + \int_{\mathbb{R}_+} N_k(v, w, Q) \phi(t, 0) dt \geq 0. \quad (25)$$

Conditions (25) originate from the classical definition of entropy solutions to hyperbolic systems of conservation laws, [34, 36]. The entropies  $E_k$  are not convex with respect to the variables  $(v, w)$  (they are convex only with respect to the conservative variable  $\rho$ ); however, given any Riemann datum not involving the vacuum state, the entropy inequalities (25) select precisely the solutions prescribed by the Aw-Rascle and Zhang Riemann solver.

We recall the existence results for unconstrained Cauchy problem (23a), and (23c) obtained in [27] away from the vacuum and in [31, 37] for solutions attaining also the vacuum state.

Some remarks on  $N_k$  are in order. First,  $N_k$  compensates the possible additional entropy dissipation at  $x = 0$  due to the constraint. Second, it makes sense to consider the traces  $f(v, w)(t, 0^\pm)$  and  $w(t, 0^\pm)$ . This is obvious as we assume that the solution  $(v, w)$  is in  $\mathbf{L}^\infty(\mathbb{R}_+; \mathbf{BV}(\mathbb{R}; \mathscr{W}))$ ; therefore we can introduce both the left measure theoretic trace  $(v, w)(t, 0^-)$ , implicitly defined by

$$\lim_{\varepsilon \downarrow 0} \frac{1}{\varepsilon} \int_{\mathbb{R}_+} \int_{-\varepsilon}^0 \|v(t, x) - v(t, 0^-)\| \phi(t, x) \, dx \, dt = 0 \quad \text{for all } \phi \in \mathbf{C}_c^\infty(\mathbb{R}^2; \mathbb{R}),$$

$$\lim_{\varepsilon \downarrow 0} \frac{1}{\varepsilon} \int_{\mathbb{R}_+} \int_{-\varepsilon}^0 \|w(t, x) - w(t, 0^-)\| \phi(t, x) \, dx \, dt = 0 \quad \text{for all } \phi \in \mathbf{C}_c^\infty(\mathbb{R}^2; \mathbb{R}),$$

and the right measure theoretic trace  $(v, w)(t, 0^+)$ , which is defined analogously. Moreover, if  $w(t, 0^-)$  and  $w(t, 0^+)$  differ then  $x \mapsto (v, w)(t, x)$  has a stationary contact discontinuity at  $x = 0$  and therefore  $N_k(v, w, Q) = 0$  because  $f(v, w)(t, 0^\pm) = 0$ .

Condition (25) does not ensure uniqueness of solutions involving a vacuum state. For this reason at vacuum, we adopt the selection criterion for **BV**-entropy solutions requiring that for any  $t > 0$  and  $x \in \mathbb{R}$

$$\left( \begin{array}{c} v(t, x^-) \\ w(t, x^-) \\ v(t, x^+) \\ w(t, x^+) \end{array} \right) \in \left\{ \left( \begin{array}{c} v_\ell \\ w_\ell \\ v_r \\ w_r \end{array} \right) \in \mathscr{W}^2 : \begin{array}{l} (v_\ell, w_\ell) \in \mathscr{W}_0 \\ (v_r, w_r) \in \mathscr{W}_0 \\ (v_\ell, w_\ell) \in \mathscr{W}_0^c \\ (v_r, w_r) \in \mathscr{W}_0 \end{array} \right\} \Rightarrow \left( \begin{array}{c} v_\ell \\ w_\ell \end{array} \right) = \left( \begin{array}{c} v_r \\ w_r \end{array} \right) \right\}. \quad (26)$$

*Remark 1* The solutions we consider in this section, and in general all solutions associated to constant or piecewise constant in time constraints and **BV**-regular initial conditions, are in  $\mathbf{L}^\infty(\mathbb{R}_+; \mathbf{BV}(\mathbb{R}; \mathscr{W}))$ ; see [6]. However since  $N_k$  can be written as the product of  $f(v, w)$  by a function of  $w$  and  $Q$ , and  $w$  enjoys the renormalization property, [41], the weak traces at  $x = 0$  of  $N_k = N_k(v, w, Q)$  exist; see [1, 6] for details. This property gives hope to extend the existence results presented here to general time-variable constraints and then to nonlocal constraints, in the spirit of the LWR-based models discussed in Sect. 2.

We collect the basic properties of constrained entropy solutions in the following.

**Proposition 2** *If  $(v, w)$  is a constrained entropy solution of (23), then:*

1. Any discontinuity of  $Y(v, w)$  satisfies the Rankine-Hugoniot jump conditions.
2. Any discontinuity of  $Y(v, w)$  away from  $x = 0$  satisfies the classical Lax entropy inequalities.
3. If  $x \mapsto Y(v, w)(t_0, x)$ ,  $t_0 > 0$ , has a nonclassical shock discontinuity, then  $f(v, w)(t_0, 0^\pm) = Q(t_0)$ .

Denote by **PC** the set of piecewise constant functions with a finite number of jumps. Let  $(\tilde{v}(Q), \tilde{w}(Q))$  be the point of the curve  $f(v, w) = Q$  with the lowest  $w$  coordinate,  $J: (0, \infty) \times \mathbb{R}_+ \rightarrow \mathbb{R}_+$  be defined by

$$J(Q, w) = \begin{cases} \check{v}(Q, w) - \hat{v}(Q, w) & \text{if } w \in [\tilde{w}(Q), \infty), \\ 0 & \text{if } w \in [0, \tilde{w}(Q)), \end{cases}$$

and for any  $w \geq \tilde{w}(Q)$ , let

$$\begin{aligned} \hat{v}(Q, w) &= \min \{v \in (0, w) : \tau(v, w) v = Q\}, \\ \check{v}(Q, w) &= \max \{v \in (0, w) : \tau(v, w) v = Q\}. \end{aligned}$$

Notice that  $\tilde{v}(Q)^2/Q = p'(Q/\tilde{v}(Q))$  and  $\tilde{w}(Q) = \tilde{v}(Q) + p(Q/\tilde{v}(Q))$ .

**Theorem 4** *Let  $(v_0, w_0) \in \mathbf{BV}(\mathbb{R}; \mathscr{W})$  satisfy (26) and  $Q \in \mathbf{PC}(\mathbb{R}_+; \mathbb{R}_+)$  be such that  $x \mapsto J(Q(0), w_0(x))$  has bounded total variation in  $\mathbb{R}_-$  and*

$$K_0 = \sum_{\substack{t > 0 \text{ s.t.} \\ Q(t^-) \neq Q(t^+)}} \sup_{y \in \mathbb{R}_-} |\text{TV}(J(Q(t^-), w_0); (-\infty, y]) - \text{TV}(J(Q(t^+), w_0); (-\infty, y])|$$

*is bounded. Then constrained Cauchy problem (23) admits a constrained entropy solution  $(v, w) \in \mathbf{C}^0(\mathbb{R}_+; \mathbf{BV}(\mathbb{R}; \mathscr{W}))$  and for all  $t, s \in \mathbb{R}_+$*

$$\text{TV}((v, w)(t)) \leq C, \quad \|(v, w)(t) - (v, w)(s)\|_{\mathbf{L}^1} \leq L |t - s|, \quad \|(v, w)(t)\|_{\mathbf{L}^\infty} \leq V_0,$$

where

$$\begin{aligned} V_0 &= \|(v_0, w_0)\|_{\mathbf{L}^\infty(\mathbb{R})}, \quad L = C \max \left\{ V_0, p^{-1}(V_0) p' \left( p^{-1}(V_0) \right) \right\} \\ C &= \text{TV}(v_0, w_0) + 3\text{TV} \left( J(Q(0), w_0); \mathbb{R}_- \right) + 2V_0 + 3(K_1 + K_2). \end{aligned}$$

Above,  $K_1$  and  $K_2$  are constants that may depend on  $K_0$ .

The proof is based on the WFT algorithm restarted at every time  $Q$  has a jump. The main obstacle for generalizing the existence result to general time-dependent  $Q$  is the dependence of the Temple functional on  $Q$  via  $J(Q, \cdot)$ .

### 3.2 Example

In this section we apply model (23) to simulate the traffic on a road in the presence of a traffic light placed at  $x = 0$ . More specifically, let  $w_2 > w_1 > 0$ , and consider two types of vehicles, the “slow vehicles” characterized by the Lagrangian marker  $w_1$  and the “fast vehicles” characterized by the Lagrangian marker  $w_2$ . Observe that the maximum speed of the fast vehicles is  $w_2$  and that one of the slow vehicles is  $w_1$ . Moreover, the length of the fast vehicles,  $1/p^{-1}(w_2)$ , is lower than that one of the slow vehicles,  $1/p^{-1}(w_1)$ ; see Fig. 6.

Place at  $x = 0$  a traffic light that turns from red to green at time  $t = 0$ . Assume that at time  $t = 0$  all the vehicles are at rest in  $[x_1, 0)$ ; more precisely, assume that the slow vehicles are uniformly distributed in  $[x_1, x_2]$  with density  $p^{-1}(w_1)$  and the fast vehicles are uniformly distributed in  $[x_2, 0)$  with density  $p^{-1}(w_2)$ . The resulting problem is (23) with initial datum

$$v_0(x) = \begin{cases} w_1 & \text{if } x \leq x_1, \\ 0 & \text{if } x_1 \leq x < 0, \\ w_2 & \text{if } x > 0, \end{cases} \quad w_0(x) = \begin{cases} w_1 & \text{if } x \leq x_2, \\ w_2 & \text{if } x > x_2, \end{cases}$$

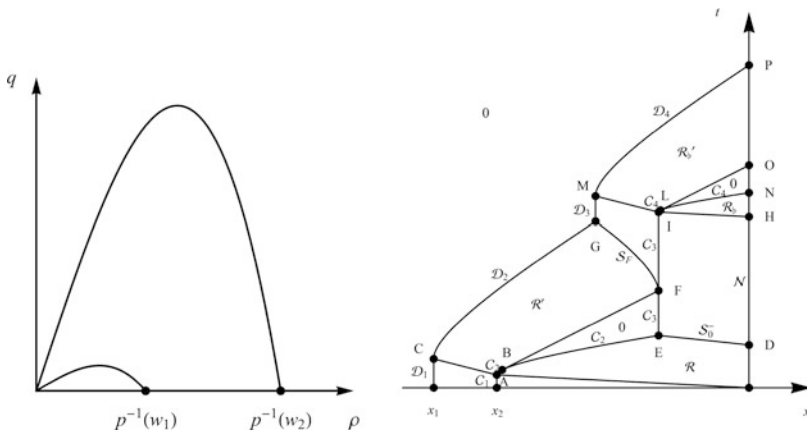


**Fig. 6** Left: The fundamental diagrams  $\rho \mapsto f(w_1 - p(\rho), w_1)$  and  $\rho \mapsto f(w_2 - p(\rho), w_2)$  corresponding to the slow and fast vehicles, respectively. Right: The solution constructed in Sect. 3.2. Above “0” stands for the vacuum

and constraint

$$Q(t) = \left( \max_{\rho \in [0, p^{-1}(w_2)]} f(w_2 - p(\rho), w_2) \right) \chi_{(0, t_D) \cup (t_H, t_P)}(t).$$

The above expression for  $Q$  means that the traffic light is green for  $t \in (0, t_D) \cup (t_H, t_P)$ ; otherwise it is red.

Below we furnish a detailed construction of the resulting solution; see Figs. 6 and 7. We first consider three Riemann problems at  $(t, x) \in \{0\} \times \{x_1, x_2, 0\}$  and obtain that from  $x = x_1$  starts a stationary discontinuity  $\mathcal{D} = \mathcal{D}_1$  from the vacuum state  $(w_1, w_1)$  to  $(0, w_1)$ , from  $x = x_2$  starts a stationary contact discontinuity  $\mathcal{C} = \mathcal{C}_1$  from  $(0, w_1)$  to  $(0, w_2)$ , and from  $x = 0$  starts a rarefaction  $\mathcal{R}$  centered in  $(t, x) = (0, 0)$  and taking values

$$\mathcal{R}: \quad \rho_{\mathcal{R}}(x/t) = \mathfrak{R}(w_2 - x/t), \quad w_{\mathcal{R}}(x/t) = w_2, \quad \text{for } x/t \in [\lambda_1(0, w_2), w_2],$$

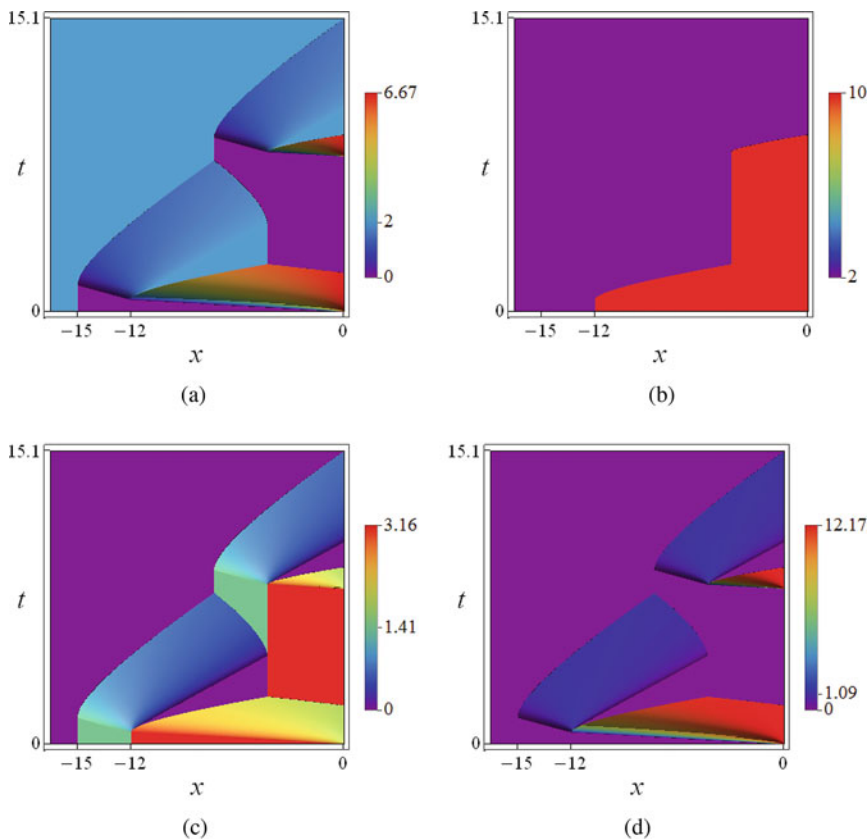


**Fig. 7** The solution constructed in Sect. 3.2. **(a)**  $(t, x) \mapsto v(t, x)$ . **(b)**  $(t, x) \mapsto w(t, x)$ . **(c)**  $(t, x) \mapsto \rho(t, x)$ . **(d)**  $(t, x) \mapsto f(t, x)$

where  $\mathfrak{X}$  is the inverse function of  $\rho \mapsto p(\rho) + \rho p'(\rho)$ . Let then

$$\begin{aligned} \mathcal{D} = \mathcal{D}_1: & & x_{\mathcal{D}_1}(t) &= x_1, \\ \mathcal{C} = \mathcal{C}_1: & & x_{\mathcal{C}_1}(t) &= x_2. \end{aligned}$$

We prolong then the solution by considering the Riemann problems at each interaction as follows:

- The contact discontinuity  $\mathcal{C}$  starts to interact with the rarefaction  $\mathcal{R}$  from  $A = (t_A, x_A) = (x_2/\lambda_1(0, w_2), x_2)$ ; as a result,  $\mathcal{C}$  accelerates according to the following ordinary differential equation

$$\mathcal{C} = \mathcal{C}_2: \quad \dot{x}_{\mathcal{C}_2}(t) = v_{\mathcal{R}}(x_{\mathcal{C}_2}(t)/t), \quad x_{\mathcal{C}_2}(t_A) = x_A. \quad (27)$$

The contact discontinuity  $\mathcal{C}$  stops to interact with the rarefaction  $\mathcal{R}$  at  $B = (t_B, x_B)$  implicitly given by  $x_B = x_{\mathcal{C}_2}(t_B)$  and  $v_{\mathcal{R}}(x_B/t_B) = w_1$ ; then the vacuum state  $(w_1, w_1)$  appears in  $\{(t, x): x_B + (t - t_B)w_1 < x < x_{\mathcal{C}_2}(t)\}$ . Observe that (27) still holds after time  $t = t_B$  because the speed of propagation of any discontinuity from any vacuum state to  $(v_*, w_*) \in \mathcal{W}_0^c$  is  $v_*$ . Notice that  $\mathcal{C}$  is not a contact discontinuity after time  $t = t_B$ .

- Each point of  $\mathcal{C}(t)$ ,  $t_A \leq t \leq t_B$ , is the center of a rarefaction appearing on its left. Denote by  $\mathcal{R}'$  the juxtaposition of these rarefactions. In order to compute the values attained by  $\mathcal{R}'$ , it is sufficient to recall that the velocity  $v$  is conserved across the contact discontinuity  $\mathcal{C}(t)$ ,  $t_A \leq t \leq t_B$ , and that the density  $\rho$  in  $\mathcal{R}'$  is constant along

$$\mathcal{P}: \quad x = x_{\mathcal{C}_2}(t_0) + \lambda_1(v_{\mathcal{R}}(x_{\mathcal{C}_2}(t_0)/t_0), w_1)(t - t_0). \quad (28)$$

Hence, the value of  $\rho_{\mathcal{R}'}$  at any point  $(t, x)$  of the rarefaction  $\mathcal{R}'$  is equal to  $\tau(v_{\mathcal{R}}, w_1)$  computed at the point  $(t_0, x_{\mathcal{C}_2}(t_0))$ , with  $t_0 = \mathcal{P}(t, x)$ , obtained by projecting  $(t, x)$  to a point of  $\mathcal{C}$  along (28):

$$\mathcal{R}': \quad \rho_{\mathcal{R}'}(t, x) = p^{-1}(w_1 - v_{\mathcal{R}}(x_{\mathcal{C}_2}(\mathcal{P}(t, x))/\mathcal{P}(t, x))), \quad w_{\mathcal{R}'}(t, x) = w_1.$$

Observe that by definition  $\mathcal{P}(t, x) \in [t_A, t_B]$  for all  $(t, x)$  in  $\mathcal{R}'$ .

- The rarefaction  $\mathcal{R}'$  reaches the stationary discontinuity  $\mathcal{D}$  in  $C = (t_C, x_C) = (t_A + (x_1 - x_2)/\lambda_1(0, w_1), x_1)$ . As a result of its interaction with  $\mathcal{R}'$ , the discontinuity  $\mathcal{D}$  starts to accelerate

$$\mathcal{D} = \mathcal{D}_2: \quad \dot{x}_{\mathcal{D}_2}(t) = v_{\mathcal{R}'}(t, x_{\mathcal{D}_2}(t)), \quad x_{\mathcal{D}_2}(t_C) = x_C.$$

- At time  $t = t_D$ , such that  $t_D > t_B$  and  $\mathcal{C}_2(t_D) < 0$ , the traffic light turns to red. Hence, at  $D = (t_D, 0)$ , the solution has a shock  $\mathcal{S}_0^-$  with negative speed, a stationary nonclassical shock  $\mathcal{N}$  from  $(0, w_2)$  to the vacuum state  $(w_2, w_2)$ , and

a shock  $\mathcal{S}_0^+$  with positive speed. Since  $\mathcal{S}_0^-$  and  $\mathcal{S}_0^+$  interact with the rarefaction  $\mathcal{R}$ , we have that

$$\begin{aligned} \mathcal{S}_0^-: \quad \dot{x}_{\mathcal{S}_0^-}(t) &= \frac{q_{\mathcal{R}}(x_{\mathcal{S}_0^-}(t)/t)}{\rho_{\mathcal{R}}(x_{\mathcal{S}_0^-}(t)/t) - p^{-1}(w_2)}, & x_{\mathcal{S}_0^-}(t_D) &= 0, \\ \mathcal{S}_0^+: \quad \dot{x}_{\mathcal{S}_0^+}(t) &= v_{\mathcal{R}}(x_{\mathcal{S}_0^+}(t)/t), & x_{\mathcal{S}_0^+}(t_D) &= 0. \end{aligned}$$

- The discontinuity  $\mathcal{C}$  and the shock  $\mathcal{S}_0^-$  meet in  $E$ , which is implicitly given by  $x_{\mathcal{C}_2}(t_E) = x_E = x_{\mathcal{S}_0^-}(t_E)$ . Observe that

$$x_E = x_2 + \frac{t_D}{p^{-1}(w_2)} \max \{f(w_2 - p(\rho), w_2) : \rho \in [0, p^{-1}(w_2)]\}.$$

As a result of this interaction,  $\mathcal{S}_0^-$  disappears and  $\mathcal{C}$  becomes stationary

$$\mathcal{C} = \mathcal{C}_3: \quad x_{\mathcal{C}_3}(t) = x_E.$$

- The discontinuity  $\mathcal{C}$  meets again the rarefaction  $\mathcal{R}'$  in  $F = (t_F, x_F) = (t_B + (x_E - x_B)/w_1, x_E)$ . As a result of this interaction, from  $F$  starts a backward shock  $\mathcal{S}_F$ , while  $\mathcal{C}$  becomes a stationary contact discontinuity. Since  $\mathcal{S}_F$  interacts with  $\mathcal{R}'$ , we have that

$$\mathcal{S}_F: \quad \dot{x}_{\mathcal{S}_F}(t) = f_{\mathcal{R}'}(t, x_{\mathcal{S}_F}(t)) / (\rho_{\mathcal{R}'}(t, x_{\mathcal{S}_F}(t)) - p^{-1}(w_1)), \quad x_{\mathcal{S}_F}(t_F) = x_F.$$

- The discontinuity  $\mathcal{D}$  and the shock  $\mathcal{S}_F$  meet in  $G$ , which is implicitly given by  $x_{\mathcal{D}_2}(t_G) = x_G = \mathcal{S}_F(t_G)$ . Observe that  $x_G = (x_1 - x_2) + x_E$ . As a result of this interaction,  $\mathcal{S}_F$  disappears and  $\mathcal{D}$  becomes stationary

$$\mathcal{D} = \mathcal{D}_3: \quad x_{\mathcal{D}_3}(t) = x_G.$$

- If at time  $t = t_H$ , with  $t_H > t_G$ , the traffic light turns to green. Then we have a rarefaction  $\mathcal{R}_b$  centered in  $H = (t_H, 0)$  and taking values

$$\mathcal{R}_b: \quad \begin{cases} \rho_{\mathcal{R}_b}(t, x) = \mathfrak{R}(w_2 - x/(t - t_H)), \\ w_{\mathcal{R}_b}(t, x) = w_2, \end{cases} \quad \text{for } x/t - t_H \in [\lambda_1(0, w_2), w_2],$$

- The contact discontinuity  $\mathcal{C}$  starts to interact with the rarefaction  $\mathcal{R}_b$  in  $I = (t_I, x_I) = (t_H + \alpha t_A, \alpha x_2)$ , where  $\alpha = x_E/x_2$ . As a result, analogously to the interaction in  $A$ ,  $\mathcal{C}$  accelerates and a rarefaction  $\mathcal{R}'_b$  appears on its left. Hence

$$\mathcal{C} = \mathcal{C}_4: \quad x_{\mathcal{C}_4}(t) = \alpha x_{\mathcal{C}_2}((t - t_H)/\alpha), \tag{29}$$

$$\begin{aligned} \mathcal{P}_b: \quad & \mathcal{P}_b(t, x) = \alpha \mathcal{P}((t - t_H)/\alpha, x/\alpha) + t_H, \\ \mathcal{R}'_b: \quad & \begin{cases} \rho_{\mathcal{R}'_b}(t, x) = p^{-1} (w_1 - v_{\mathcal{R}}(x_{\mathcal{C}_4}(\mathcal{P}_b(t, x)) / (\mathcal{P}_b(t, x) - t_H))), \\ w_{\mathcal{R}'_b}(t, x) = w_1. \end{cases} \end{aligned}$$

- The contact discontinuity  $\mathcal{C}$  stops to interact with the rarefaction  $\mathcal{R}_b$  from  $L = (t_L, x_L) = (t_H + \alpha t_B, \alpha x_B)$  and the vacuum state  $(w_1, w_1)$  appears in  $\{(t, x) : x_L + (t - t_L)w_1 < x < x_{\mathcal{C}_4}(t)\}$ . Observe that (29) still holds after time  $t = t_L$ . Notice that  $\mathcal{C}$  is not a contact discontinuity after time  $t = t_L$ .
- The rarefaction  $\mathcal{R}'_b$  reaches the stationary discontinuity  $\mathcal{D}$  in  $M = (t_M, x_M) = (t_I + (x_G - x_E)/\lambda_1(0, w_1), x_G)$ . As a result of its interaction with  $\mathcal{R}'_b$ , the discontinuity  $\mathcal{D}$  starts to accelerate

$$\mathcal{D} = \mathcal{D}_4: \quad \dot{x}_{\mathcal{D}_4}(t) = v_{\mathcal{R}'_b}(t, x_{\mathcal{D}_4}(t)), \quad x_{\mathcal{D}_4}(t_M) = x_M. \quad (30)$$

- The discontinuity  $\mathcal{D}$  reaches  $x = 0$  in  $P$  implicitly given by  $x_{\mathcal{D}_4}(t_P) = x_P = 0$ .

At time  $t = t_P$  no vehicles are present in  $\mathbb{R}_-$ , and the construction of the solution in the left half-plane is concluded. In Figs. 6 and 7, we represent the solution corresponding to

$$p(\rho) = \rho^2, \quad w_1 = 2, \quad w_2 = 10, \quad x_1 = -15, \quad x_2 = -12, \quad t_D = 2, \quad t_H = 8.$$

Notice that we have the following expressions for  $\mathcal{D}$  and  $\mathcal{C}$ :

$$x_{\mathcal{D}}(t) = x_1 \chi_{[0, t_C]}(t) + x_{\mathcal{D}_2}(t) \chi_{[t_C, t_G]}(t) + x_G \chi_{[t_G, t_M]}(t) + x_{\mathcal{D}_4}(t) \chi_{[t_M, +\infty]}(t),$$

$$x_{\mathcal{C}}(t) = x_2 \chi_{[0, t_A]}(t) + x_{\mathcal{C}_2}(t) \chi_{[t_A, t_F]}(t) + x_E \chi_{[t_F, t_I]}(t) + x_{\mathcal{C}_4}(t) \chi_{[t_I, +\infty]}(t).$$

In order to compute time  $t_P$ , we can exploit the equation

$$\int_{x_{\mathcal{D}_4}(t)}^0 \rho_{\mathcal{R}'_b}(t, y) dy + \int_{t_0}^t f_{\mathcal{R}'_b}(s, 0) ds = p^{-1}(w_1)(x_2 - x_1), \quad t \in [t_0, t_P],$$

to obtain an alternative way to compute  $t_P$  given by solving the following equation:

$$t_P: \quad \int_{t_0}^{t_P} f_{\mathcal{R}'_b}(t, 0) dt = p^{-1}(w_1)(x_2 - x_1).$$

The above equation allows to compute  $t_P$  by solving (29) for times  $t \in [t_I, t_L]$  instead of (30) for times  $t \in [t_M, t_P]$ , that is computationally much more expensive.



### 4 Locally Constrained PT

In this section we study the Cauchy problem for PT (3), and (4) subject to a point constraint on the density flow (5). More precisely, with the same notations used in the previous sections, we describe the traffic in the *free-flow phase*  $\Omega_f$  with constrained LWR (6) and the traffic in the *congested phase*  $\Omega_c$  with constrained ARZ (23). The coupling is achieved via *phase transitions*, namely, discontinuities that separate two states belonging to different phases and that satisfy the Rankine-Hugoniot conditions.

We point out that in [11, 12, 20, 30], it is assumed that  $\Omega_f \cap \Omega_c = \emptyset$ , while in [13, 14], it is assumed that  $\Omega_f \cap \Omega_c \neq \emptyset$ . Moreover, in [13, 14], it is assumed that the flux function vanishes at a maximal density, namely, that the vehicles have (almost) the same length, while in [11, 12, 30], this requirement is not assumed. Here we assume that  $\Omega_f \cap \Omega_c \neq \emptyset$  and, in order to ensure the well-posedness of the Cauchy problems, see [20, Remark 2], we also assume that  $\Omega_f$  is characterized by a unique value of the velocity,  $V \equiv V_{\max}$ . At last, we consider a heterogeneous traffic with vehicles having different lengths. As a consequence

$$\Omega_f = \Omega_f^- \cup \Omega_f^+, \quad \Omega_c = \{(\tau(v, w), v) \in \mathbb{R}_+ \times [0, V_{\max}] : w \in [W^-, W^+]\},$$

where

$$\Omega_f^- = [0, \sigma_-) \times \{V_{\max}\}, \quad \Omega_f^+ = [\sigma_-, \sigma_+] \times \{V_{\max}\},$$

with  $\sigma_{\pm} = \tau(V_{\max}, W^{\pm})$  and  $0 < V_{\max} < W^- < W^+$  are such that

$$V_{\max} < p^{-1}(W^- - V_{\max}) p'(p^{-1}(W^- - V_{\max})).$$

Notice that  $\Omega_f^+ = \Omega_f \cap \Omega_c$  is the *metastable phase* and is not empty.

This two-phase approach is motivated by experimental observations, according to which for low densities the flow of vehicles is approximable by a one-dimensional manifold as  $\Omega_f$ , while at high densities, the flow covers a two-dimensional manifold as  $\Omega_c$ ; see [20, Figure 1.1] or [14, Figure 3.1].

We introduce the following functions:

$$\begin{aligned} w : \Omega &\rightarrow [0, W^+], & w(\rho, v) &= \begin{cases} p(\rho) + v & \text{if } (\rho, v) \in \Omega_c, \\ W^- - \rho/\sigma_- & \text{if } (\rho, v) \in \Omega_f^-, \end{cases} \\ W : \Omega &\rightarrow [W^-, W^+], & W(\rho, v) &= \max\{W^-, w(\rho, v)\}, \\ f : \Omega &\rightarrow \mathbb{R}_+, & f(\rho, v) &= \rho v. \end{aligned}$$

We consider the Cauchy problem for PT (3), and (4)

**Free flow**

**Congested flow**

$$\begin{cases} u=(\rho, v) \in \Omega_f, \\ \rho_t + f(\rho, v)_x = 0, \\ v=V_{\max}, \end{cases} \quad \begin{cases} u=(\rho, v) \in \Omega_c, \\ \rho_t + f(\rho, v)_x=0, \\ [\rho w(\rho, v)]_t + [f(\rho, v) w(\rho, v)]_x = 0, \end{cases} \quad u(0, x)=u_0(x), \tag{31}$$

subject to a point constraint on the density flow (5)

$$f(\rho, v)(t, 0^\pm) \leq Q, \tag{32}$$

where  $u_0 \in \mathbf{L}^\infty(\mathbb{R}; \Omega)$  is the initial datum and  $Q$  is the constant maximal density flow allowed at  $x = 0$ . Clearly, as in [11, 12, 24, 30], the traffic is described by LWR in the free-flow phase and ARZ in the congested phase.

Let  $f_c^\pm = \sigma_\pm V_{\max}$ . Introduce  $V_Q^\pm \in [0, V_{\max}]$  and  $W_Q \in [0, W^+]$  defined by the following conditions:

if  $Q = f_c^+$  :

$$V_Q^+ = V_{\max}, \quad V_Q^- = V_{\max}, \quad W_Q = W^+,$$

if  $Q \in [f_c^-, f_c^+)$  :

$$V_Q^+ = V_{\max}, \quad V_Q^- + p\left(\frac{Q}{V_Q^-}\right) = W^+, \quad W_Q = p\left(\frac{Q}{V_{\max}}\right) + V_{\max},$$

if  $Q \in (0, f_c^-)$  :

$$V_Q^+ + p\left(\frac{Q}{V_Q^+}\right) = W^-, \quad V_Q^- + p\left(\frac{Q}{V_Q^-}\right) = W^+, \quad W_Q = \frac{Q}{f_c^-},$$

if  $Q = 0$  :

$$V_Q^+ = 0, \quad V_Q^- = 0, \quad W_Q = 0.$$

For any  $Q \in (0, f_c^+)$ , let  $\Xi_Q : [V_Q^-, V_Q^+] \rightarrow [W^-, W^+]$  be given by  $\Xi_Q(v) = v + p(Q/v)$ . Notice that  $\Xi_Q$  is strictly decreasing and strictly convex.

### 4.1 Existence Result

Before stating the definition of entropy solution to (31), we introduce the family of entropy-entropy flux pairs

$$E_k(\rho, v) = \begin{cases} 0 & \text{if } v \geq k, \\ \frac{\rho}{p^{-1}(W(\rho, v) - k)} - 1 & \text{if } v < k, \end{cases} \quad F_k(\rho, v) = \begin{cases} 0 & \text{if } v \geq k, \\ \frac{f(\rho, v)}{p^{-1}(W(\rho, v) - k)} - k & \text{if } v < k. \end{cases}$$

**Definition 4** We say that  $(\rho, v) \in \mathbf{L}^\infty(\mathbb{R}_+; \mathbf{BV}(\mathbb{R}; \Omega)) \cap \mathbf{C}^0(\mathbb{R}_+; \mathbf{L}_{\text{loc}}^1(\mathbb{R}; \Omega))$  is a constrained entropy solution to (31), and (32) if the following conditions holds:

- (i)  $(\rho, v)$  is a weak solution to Cauchy problem (31), i.e.,  $(\rho, v)(0, x) = (\rho_0, v_0)(x)$  for a.e.  $x \in \mathbb{R}$ , and for any test function  $\phi \in \mathbf{C}_c^\infty((0, \infty) \times \mathbb{R}; \mathbb{R})$ , we have

$$\iint_{\mathbb{R}_+ \times \mathbb{R}} (\rho \phi_t + f(\rho, v) \phi_x) \, dx \, dt = 0 \tag{33}$$

and if  $\phi(\cdot, 0) \equiv 0$ , then

$$\iint_{\mathbb{R}_+ \times \mathbb{R}} (\rho \phi_t + f(\rho, v) \phi_x) \mathbb{W}(\rho, v) \, dx \, dt = 0. \tag{34}$$

- (ii)  $(\rho, v)$  satisfies constraint (32), namely,  $f(\rho, v)(t, 0_\pm) \leq Q$  for a.e.  $t > 0$  and for any test function  $\phi \in \mathbf{C}_c^\infty((0, \infty) \times \mathbb{R}; \mathbb{R}_+)$  such that  $\phi(\cdot, 0) \equiv 0$  and constant  $k \in [0, V_{\max}]$

$$\iint_{\mathbb{R}_+ \times \mathbb{R}} (\mathbb{E}_k(\rho, v) \phi_t + Q_k(\rho, v) \phi_x) \, dx \, dt \geq 0. \tag{35}$$

In the following proposition, we state which discontinuities are admissible for constrained entropy solutions.

**Proposition 3** *If  $(\rho, v)$  is a constrained entropy solution of (31), and (32), then:*

- Any discontinuity  $\delta(t)$  of  $x \mapsto (\rho, v)(t, x)$  satisfies the first Rankine-Hugoniot jump condition

$$\left[ \rho(t, \delta(t)_+) - \rho(t, \delta(t)_-) \right] \dot{\delta}(t) = f(\rho, v)(t, \delta(t)_+) - f(\rho, v)(t, \delta(t)_-), \tag{36}$$

and if  $\delta(t) \neq 0$ , then it satisfies also the second Rankine-Hugoniot jump condition

$$\begin{aligned} & \left[ \rho(t, \delta(t)_+) \mathbb{W}(\rho, v)(t, \delta(t)_+) - \rho(t, \delta(t)_-) \mathbb{W}(\rho, v)(t, \delta(t)_-) \right] \dot{\delta}(t) \\ &= f(\rho, v)(t, \delta(t)_+) \mathbb{W}(\rho, v)(t, \delta(t)_+) - f(\rho, v)(t, \delta(t)_-) \mathbb{W}(\rho, v)(t, \delta(t)_-). \end{aligned} \tag{37}$$

- Any discontinuity of  $(\rho, v)$  away from the constraint satisfies the Lax entropy inequalities.
- Nonclassical discontinuities of  $(\rho, v)$  may occur only at the constraint location  $x = 0$ , and in this case, the density flux at  $x = 0$  does not exceed the maximal flux  $Q$  allowed by the constraint.

*Remark 2* In (34) and (35), we consider test functions  $\phi$  such that  $\phi(\cdot, 0) \equiv 0$ . Indeed a constrained entropy solution  $(\rho, v)$  to constrained Cauchy problem (31), and (32) does not satisfy in general second Rankine-Hugoniot condition (37) along  $x = 0$

$$f(\rho, v)(t, 0_-) W(\rho, v)(t, 0_-) = f(\rho, v)(t, 0_+) W(\rho, v)(t, 0_+) \quad \text{for a.e. } t > 0.$$

Therefore, even if  $(\rho, v)$  takes values in  $\Omega_c$ , it may not be a weak solution to ARZ (23).

This is in the same spirit of the solutions considered in [12, 24, 28] for traffic through locations with reduced capacity. This choice for the test functions in (34) and (35) does not allow us to better characterize the (density) flux at  $x = 0$  associated to nonclassical shocks. In particular, different from what is proved in Sect. 2 for constrained LWR and Sect. 3 for constrained ARZ, we cannot ensure that the flux of the nonclassical shocks of  $(\rho, v)$  is equal to  $Q$ .

Let the maps  $[0, W^+] \ni w \mapsto \hat{u}(w) = (\hat{\rho}(w), \hat{v}(w)) \in \Omega_c$  and  $[0, V_{\max}] \ni v \mapsto \check{u}(v) = (\check{\rho}(v), \check{v}(v)) \in \Omega$  be defined in the  $(v, w)$  coordinates by

$$\hat{v}(w) = \begin{cases} \Xi_Q^{-1}(w) & \text{if } w > \max\{W^-, W_Q\}, \\ V_Q^+ & \text{if } W_Q < w \leq W^-, \\ V & \text{if } w \leq W_Q, \end{cases} \quad \check{v}(v) = \begin{cases} V & \text{if } v > V_Q^+, \\ v & \text{if } v \in [V_Q^-, V_Q^+], \\ V_Q^- & \text{if } v < V_Q^-, \end{cases}$$

$$\hat{w}(w) = \begin{cases} w & \text{if } w > \max\{W^-, W_Q\}, \\ W^- & \text{if } W_Q < w \leq W^-, \\ W_Q & \text{if } w \leq W_Q, \end{cases} \quad \check{w}(v) = \begin{cases} W_Q & \text{if } v > V_Q^+, \\ \Xi_Q(v) & \text{if } v \in [V_Q^-, V_Q^+], \\ W^+ & \text{if } v < V_Q^-. \end{cases}$$

Notice that

$$f(\hat{u}(w)) = f(\check{u}(v)) = Q.$$

Denote by  $\text{TV}_+$  and  $\text{TV}_-$  are the positive and negative total variations, respectively. For any  $u = (\rho, v): \mathbb{R} \rightarrow \Omega$ , let

$$\hat{\Upsilon}(u) = \text{TV}_+(\hat{v}(w(u)); (-\infty, 0)) + \text{TV}_-(\hat{w}(w(u)); (-\infty, 0)),$$

$$\check{\Upsilon}(u) = \text{TV}_+(\check{v}(v); (0, \infty)) + \text{TV}_-(\check{w}(v); (0, \infty)).$$

We are now in the position to state the main result of the paper.

**Theorem 5** *Let  $(\rho_0, v_0) \in \mathbf{L}^1 \cap \mathbf{BV}(\mathbb{R}; \Omega)$  and  $Q \in [0, f_c^+]$  satisfy one of the following conditions:*

- (i)  $Q \in [f_c^-, f_c^+]$ ;
- (ii)  $Q \in [0, f_c^-)$  and  $\hat{\Upsilon}(\rho_0, v_0) + \check{\Upsilon}(\rho_0, v_0)$  is bounded.

Then constrained Cauchy problem (31), and (32) admits a constrained entropy solution  $(\rho, v) \in \mathbf{L}^\infty(\mathbb{R}_+; \mathbf{BV}(\mathbb{R}; \Omega)) \cap \mathbf{C}^0(\mathbb{R}_+; \mathbf{L}_{\text{loc}}^1(\mathbb{R}; \Omega))$  and for all  $t, s \in \mathbb{R}_+$

$$\text{TV}(u(t)) \leq C, \quad \|u(t) - u(s)\|_{\mathbf{L}^1} \leq L|t - s|, \quad \|u(t)\|_{\mathbf{L}^\infty} \leq p^{-1}(W^+) + V_{\max},$$

where  $C$  and  $L$  are constants that depend on  $(\rho_0, v_0)$  and  $Q$ .

The proof is based on the WFT algorithm; see [10] for the details. Let us just underline that if  $Q \in [f_c^-, f_c^+]$ , then  $w \mapsto \hat{u}(w)$  and  $v \mapsto \check{u}(v)$  are Lipschitz continuous, and therefore  $\hat{\Upsilon}(\rho_0, v_0) + \hat{\Upsilon}(\rho_0, v_0)$  is bounded if  $(\rho_0, v_0)$  has bounded total variation. On the other hand, if  $Q < f_c^-$ , then  $w \mapsto \hat{u}(w)$  and  $v \mapsto \check{u}(v)$  are only left-continuous. This motivates the differences between the hypotheses (i) and (ii) of Theorem 5.

### 4.2 Example

In this section we apply model (31), and (32) to simulate the traffic on a road in the presence of an obstacle, such as a construction site, with capacity  $Q$  and placed at  $x = 0$ ; see Fig. 8. More specifically, let  $w_2 \in (W^-, W^+)$  be the Lagrangian marker corresponding to vehicles that are initially at rest in  $[x_2, 0)$ . We place in  $[x_1, x_2)$  vehicles with density  $\rho_1 \in (0, \sigma_-)$ ; these vehicles clearly move with speed  $V_{\max}$ . The resulting initial condition is

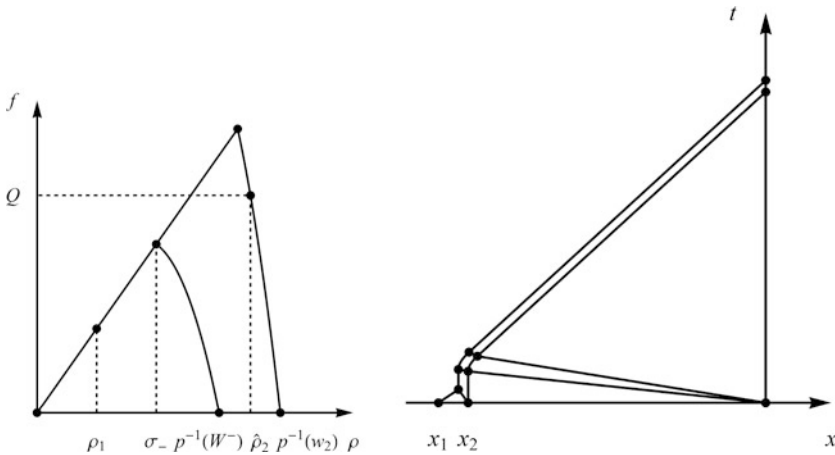


**Fig. 8** Left: The fundamental diagrams  $\rho \mapsto f(W^- - p(\rho), w_1)$  and  $\rho \mapsto f(w_2 - p(\rho), w_2)$ . Right: The solution constructed in Sect. 4.2

$$u(0, x) = \begin{cases} u_0 & \text{if } x \in \mathbb{R} \setminus [x_1, 0), \\ u_1 & \text{if } x \in [x_1, x_2), \\ u_2 & \text{if } x \in [x_2, 0) \end{cases}$$

where  $u_0 = (0, V_{\max})$ ,  $u_1 = (\rho_1, V_{\max})$  and  $u_2 = (p^{-1}(w_2), 0)$ . For times sufficiently small, the solution is the juxtaposition of the solutions to three Riemann problems at  $(t, x) \in \{0\} \times \{x_1, x_2, 0\}$  that are

$$R[u_0, u_1]\left(\frac{x - x_1}{t}\right), \quad R[u_1, u_2]\left(\frac{x - x_2}{t}\right), \quad R_Q[u_2, u_0]\left(\frac{x}{t}\right).$$

More precisely, from  $x = x_1$  starts a contact discontinuity from the vacuum state  $u_0$  to  $u_1$ , from  $x = x_2$  starts a phase transition from  $u_1$  to  $(p^{-1}(W^-), 0)$  and a

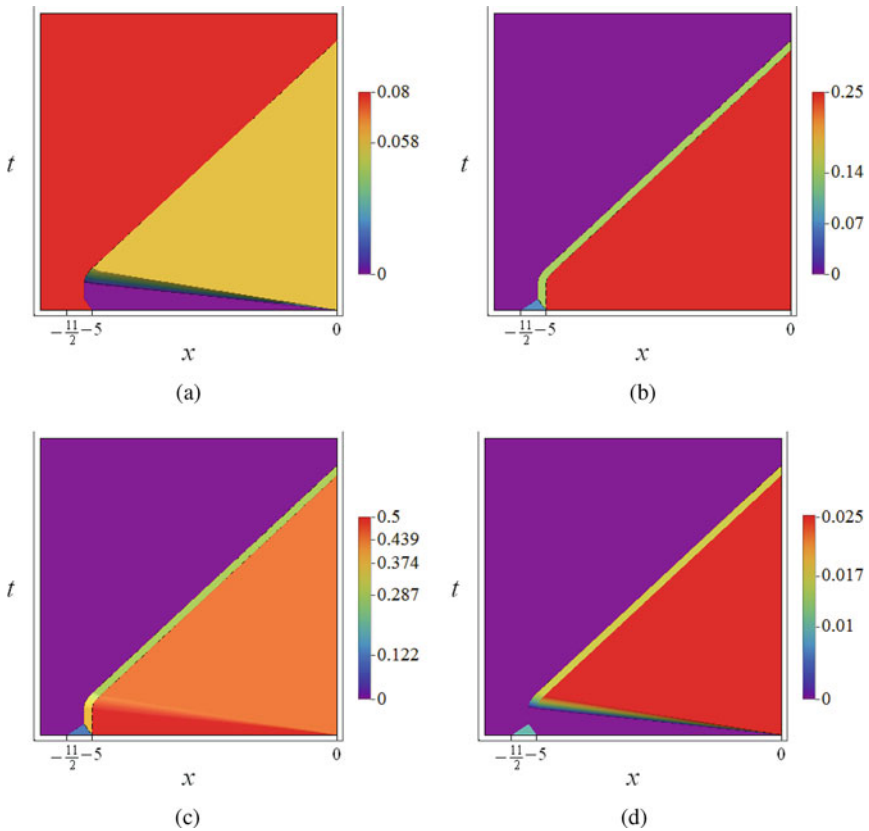


**Fig. 9** The solution constructed in Sect. 4.2. (a)  $(t, x) \mapsto v(t, x)$ . (b)  $(t, x) \mapsto w(t, x)$ . (c)  $(t, x) \mapsto \rho(t, x)$ . (d)  $(t, x) \mapsto f(t, x)$

stationary contact discontinuity from  $(p^{-1}(W^-), 0)$  to  $u_2$ , and from  $x = 0$  starts a rarefaction ranging values from  $u_2$  to  $\hat{u}(w_2, Q)$ , a (stationary) nonclassical shock from  $\hat{u}(w_2, Q)$  to  $\check{u}(V_{\max}, Q)$ , and a contact discontinuity from  $\check{u}(V_{\max}, Q)$  to  $u_0$ . The remaining construction of the solution is then similar to that described in Sect. 3.2 for the constrained ARZ. In Fig. 9 we represent the solution corresponding to

$$\begin{aligned} x_1 &= -\frac{11}{2}, & x_2 &= -5, & p(\rho) &= \rho^2, & V_{\max} &= \frac{2}{25}, \\ W^- &= \frac{7}{50}, & w_2 &= \frac{1}{4}, & \rho_1 &= \frac{\sqrt{6}}{20}, & Q &= \frac{7(31\sqrt{17} - 15)}{31250}. \end{aligned}$$

**Acknowledgements** MDR acknowledges support from Università degli Studi di Ferrara Project 2017 “FIR: Modelli macroscopici per il traffico veicolare o pedonale”.

## References

1. B. Andreianov, C. Donadello, U. Razafison, J. Y. Rolland, and M. D. Rosini. Solutions of the Aw-Rascle-Zhang system with point constraints. *Networks and Heterogeneous Media*, 11(1):29–47, 2016.
2. B. Andreianov, C. Donadello, U. Razafison, and M. D. Rosini. Riemann problems with non-local point constraints and capacity drop. *Mathematical Biosciences and Engineering*, 12(2):259–278, 2015.
3. B. Andreianov, C. Donadello, U. Razafison, and M. D. Rosini. Qualitative behaviour and numerical approximation of solutions to conservation laws with non-local point constraints on the flux and modeling of crowd dynamics at the bottlenecks. *ESAIM. Mathematical Modelling and Numerical Analysis*, 50(5):1269–1287, 2016.
4. B. Andreianov, C. Donadello, U. Razafison, and M. D. Rosini. Analysis and approximation of one-dimensional scalar conservation laws with general point constraints on the flux. *Journal de Mathématiques Pures et Appliquées*, 2018.
5. B. Andreianov, C. Donadello, and M. D. Rosini. Crowd dynamics and conservation laws with nonlocal constraints and capacity drop. *Mathematical Models and Methods in Applied Sciences*, 24(13):2685–2722, 2014.
6. B. Andreianov, C. Donadello, and M. D. Rosini. A second-order model for vehicular traffics with local point constraints on the flow. *Mathematical Models and Methods in Applied Sciences*, 26(04):751–802, 2016.
7. B. Andreianov, P. Goatin, and N. Seguin. Finite volume schemes for locally constrained conservation laws. *Numerische Mathematik*, 115(4):609–645, 2010.
8. A. Aw and M. Rascle. Resurrection of “Second Order” Models of Traffic Flow. *SIAM Journal on Applied Mathematics*, 60(3):pp. 916–938, 2000.
9. N. Bellomo and C. Dogbe. On the modeling of traffic and crowds: a survey of models, speculations, and perspectives. *SIAM Review*, 53(3):409–463, 2011.
10. M. Benyahia, C. Donadello, N. Dymski, and M. D. Rosini. An existence result for a constrained two-phase transition model with metastable phase for vehicular traffic, 2018. To appear on *Nonlinear Differential Equations and Application*. Doi: [10.1007/s00030-018-0539-1](https://doi.org/10.1007/s00030-018-0539-1)
11. M. Benyahia and M. D. Rosini. Entropy solutions for a traffic model with phase transitions. *Nonlinear Analysis: Theory, Methods & Applications*, 141:167–190, 2016.

12. M. Benyahia and M. D. Rosini. A macroscopic traffic model with phase transitions and local point constraints on the flow. *Networks and Heterogeneous Media*, 12(2):297–317, 2017.
13. S. Blandin, P. Goatin, B. Piccoli, A. Bayen, and D. Work. A general phase transition model for traffic flow on networks. *Procedia - Social and Behavioral Sciences*, 54(Supplement C):302–311, 2012. Proceedings of EWGT2012 - 15th Meeting of the EURO Working Group on Transportation, September 2012, Paris.
14. S. Blandin, D. Work, P. Goatin, B. Piccoli, and A. Bayen. A general phase transition model for vehicular traffic. *SIAM Journal on Applied Mathematics*, 71(1):107–127, 2011.
15. A. Bressan. *Hyperbolic systems of conservation laws*, volume 20 of *Oxford Lecture Series in Mathematics and its Applications*. Oxford University Press, Oxford, 2000. The one-dimensional Cauchy problem.
16. C. Cancès and N. Seguin. Error Estimate for Godunov Approximation of Locally Constrained Conservation Laws. *SIAM Journal on Numerical Analysis*, 50(6):3036–3060, 2012.
17. E. M. Cepolina. Phased evacuation: An optimisation model which takes into account the capacity drop phenomenon in pedestrian flows. *Fire Safety Journal*, 44(4):532–544, 2009.
18. C. Chalons. Numerical approximation of a macroscopic model of pedestrian flows. *SIAM Journal on Scientific Computing*, 29(2):539–555, 2007.
19. C. Chalons, P. Goatin, and N. Seguin. General constrained conservation laws. Application to pedestrian flow modeling. *Networks and Heterogeneous Media*, 8(2):433–463, 2013.
20. R. M. Colombo. Hyperbolic phase transitions in traffic flow. *SIAM Journal on Applied Mathematics*, 63(2):708–721 (electronic), 2002.
21. R. M. Colombo and P. Goatin. A well posed conservation law with a variable unilateral constraint. *Journal of Differential Equations*, 234(2):654–675, 2007.
22. R. M. Colombo, P. Goatin, and M. D. Rosini. On the modelling and management of traffic. *ESAIM: Mathematical Modelling and Numerical Analysis*, 45(05):853–872, 2011.
23. R. M. Colombo and M. D. Rosini. Pedestrian flows and non-classical shocks. *Mathematical Methods in the Applied Sciences*, 28(13):1553–1567, 2005.
24. E. Dal Santo, M. D. Rosini, N. Dymski, and M. Benyahia. General phase transition models for vehicular traffic with point constraints on the flow. *Mathematical Methods in the Applied Sciences*, 40(18):6623–6641, 2017.
25. N. S. Dymski, P. Goatin, and M. D. Rosini. Existence of BV solutions for a non-conservative constrained Aw-Rascle-Zhang model for vehicular traffic. *Journal of Mathematical Analysis and Applications*, 467(2018): 45–66. Doi:[10.1016/j.jmdd.2018.07.025](https://doi.org/10.1016/j.jmdd.2018.07.025)
26. S. Fan and B. Seibold. Data-fitted first-order traffic models and their second-order generalizations: Comparison by trajectory and sensor data. *Transportation Research Record*, 2391:32–43, 2013.
27. R. E. Ferreira and C. I. Kondo. Glimm method and wave-front tracking for the Aw-Rascle traffic flow model. *Far East Journal of Mathematical Sciences*, 43(2):203–223, 2010.
28. M. Garavello and P. Goatin. The Aw-Rascle traffic model with locally constrained flow. *Journal of Mathematical Analysis and Applications*, 378(2):634–648, 2011.
29. M. Garavello and B. Piccoli. Traffic flow on networks, volume 1 of AIMS Series on Applied Mathematics. *American Institute of Mathematical Sciences (AIMS)*, Springfield, MO, 2006.
30. P. Goatin. The Aw-Rascle vehicular traffic flow model with phase transitions. *Mathematical and computer modelling*, 44(3):287–303, 2006.
31. M. Godvik and H. Hanche-Olsen. Existence of solutions for the Aw–Rascle traffic flow model with vacuum. *Journal of Hyperbolic Differential Equations*, 05(01):45–63, 2008.
32. H. Holden and N. H. Risebro. *Front tracking for hyperbolic conservation laws*, volume 152. Springer, 2013.
33. S. N. Kruzhkov. First order quasilinear equations with several independent variables. *Matematicheskii Sbornik*, 81 (123):228–255, 1970.
34. P. D. Lax. Hyperbolic Systems of Conservation Laws II. In P. Sarnak and A. Majda, editors, *Selected Papers Volume I*, pages 233–262. Springer New York, 2005.



35. M. J. Lighthill and G. B. Whitham. On kinematic waves. II. A theory of traffic flow on long crowded roads. *Proceedings of the Royal Society. London. Series A. Mathematical, Physical and Engineering Sciences*, 229:317–345, 1955.
36. T. P. Liu. The Riemann problem for general systems of conservation laws. *Journal of Differential Equations*, 18:218–234, 1975.
37. Y.-G. Lu. Existence of global bounded weak solutions to nonsymmetric systems of Keyfitz-Kranzer type. *Journal of Functional Analysis*, 261(10):2797–2815, 2011.
38. R. Mohan and G. Ramadurai. State-of-the art of macroscopic traffic flow modelling. *International Journal of Advances in Engineering Sciences and Applied Mathematics*, 5(2–3):158–176, 2013.
39. E. Y. Panov. On sequences of measure-valued solutions of a first-order quasilinear equation. *Matematicheskii Sbornik*, 185(2):87–106, 1994.
40. E. Y. Panov. Existence of strong traces for quasi-solutions of multidimensional conservation laws. *Journal of Hyperbolic Differential Equations*, 4(4):729–770, 2007.
41. E. Y. Panov. Generalized solutions of the Cauchy problem for a transport equation with discontinuous coefficients. In *Instability in models connected with fluid flows. II*, volume 7 of *International Mathematical Series (New York)*, pages 23–84. Springer, New York, 2008.
42. B. Piccoli and A. Tosin. Vehicular traffic: A review of continuum mathematical models. In R. A. Meyers, editor, *Mathematics of Complexity and Dynamical Systems*, pages 1748–1770. Springer New York, 2011.
43. P. I. Richards. Shock waves on the highway. *Operations Research*, 4(1):pp. 42–51, 1956.
44. M. D. Rosini. *Macroscopic models for vehicular flows and crowd dynamics: theory and applications*. Understanding Complex Systems. Springer, Heidelberg, 2013.
45. V. V. Rusanov. The calculation of the interaction of non-stationary shock waves with barriers. *Akademija Nauk SSSR. Zhurnal Vychislitel'noi Matematiki i Matematicheskoi Fiziki*, 1:267–279, 1961.
46. F. van Wageningen-Kessels, H. van Lint, K. Vuik, and S. Hoogendoorn. Genealogy of traffic flow models. *EURO Journal on Transportation and Logistics*, pages 1–29, 2014.
47. Walk21-VI, editor. *Understanding capacity drop for designing pedestrian environments*, 2005.
48. H. M. Zhang. A non-equilibrium traffic model devoid of gas-like behavior. *Transportation Research Part B: Methodological*, 36(3):275 – 290, 2002.